Plio-Pleistocene intra-plate magmatism from the southern Sulu Arc, Semporna peninsula, Sabah, Borneo: Implications for high-Nb basalt in subduction zones

Colin G. Macpherson[1,2,*], Kai Kim Chiang[2,†], Robert Hall[2],
Geoff M. Nowell[1], Paterno R. Castillo[3], Matthew F. Thirlwall[4]

[1] Department of Earth Sciences, University of Durham, Durham, DH1 3LE, UK

[2] Southeast Asia Research Group, Department of Earth Sciences, Royal Holloway University of London, Egham, Surrey, TW20 0EX

[3] Geosciences Research Division, Scripps Institution of Oceanography, University of California San Diego, CA 92093-0212, USA

[4] Department of Earth Sciences, Royal Holloway University of London, Egham, Surrey, TW20 0EX

* Corresponding author:
colin.macpherson@durham.ac.uk
Tel: +44 (0)191 334 2283
Fax: +44 (0)191 334 2301

† Now at: Stockholm Environment Institute, Witthyakit Building, 254 Chulalongkorn University, Chulalongkorn Soi 64, Phyathai Road, Pathumwan, Bangkok 10330, Thailand

Revised Version Submitted to *Journal of Volcanology and Geothermal Research*
(Wysoczanski-Gamble Arc special issue)
23 September 2009

Word Count	Abstract:	320
	Text:	7089
	References:	2535 (86)
	Captions:	531
Item Count	Figures:	9
	Tables:	2

Abstract

New analyses of major and trace element concentrations and Sr, Nd and Pb isotopic ratios are presented for Plio-Pleistocene basalts and basaltic andesites from the Semporna peninsula in Sabah, Borneo, at the southern end of the Sulu Arc. Depletion of high field strength elements (HFSE), which is characteristic of many subduction-related magmatic suites, is present in more evolved Semporna rocks but is associated with radiogenic Sr and Pb, and less radiogenic Nd isotopic ratios and results from contamination of mafic melt by, possibly ancient, crustal basement. The most mafic lavas from Semporna, and elsewhere in the Sulu Arc, display no HFSE depletion relative to other elements with similar compatibility.

High-Nb basalt from Semporna formed when mantle resembling the source of Ocean Island Basalt (OIB) upwelled into lithospheric thin spots created during earlier subduction. This mantle did not experience enrichment by fluids or melt derived from subducted crust. The presence of similar lavas throughout the Sulu Arc and around the South China Sea suggests that the OIB-like component resides in the convecting upper mantle. Depletion of light rare earth elements, with respect to other incompatible elements, throughout the Sulu Arc could result from melt-mantle interaction during magma transport through the lithosphere. Such depletion is absent in suites from the South China Sea, where magma probably migrated along large, lithosphere penetrating structures.

Semporna high-Nb basalts are not associated with adakitic magmatism which is a frequent, but not ubiquitous, association in some active subduction zones. Both geochemical signatures are developed early in the history of a melt pulse, either in the source (high-Nb basalt) or during deep differentiation (adakite). Preservation of these distinctive geochemical signatures is favoured in settings that minimise (i) interaction with other, more copious melt types, or (ii) subsequent differentiation in the shallow crust. Where found, the high-Nb basalt – adakite association is a result of transport through favourable lithospheric conditions and not due to any link between their mantle sources.

Keywords: High-Nb basalt; Nb-enriched basalt; Sabah; Borneo; subduction; OIB; magmatism

1. Introduction

Subduction is an important process in generating new crust at the present time and may have played a crucial role in generating continental crust throughout much of Earth history

(Rudnick, 1995). Understanding subduction, and the crust that it produces, requires an understanding of spatial and temporal variations of magmatic products generated both within individual subduction zones and between different subduction zones. A striking feature of magmatism in modern volcanic arcs is the marked depletion of high field strength elements (HFSE, such as Nb, Zr and Ti) relative to other elements with similar compatibilities. This depletion is thought to result from differential transport of HFSE compared to other elements during recycling from the slab to the mantle wedge (Thirlwall et al., 1994). Many subduction-related basalts also possess low absolute concentrations of Nb.

Although common, relative depletion of HFSE is not ubiquitous in arc magmatism. Several subduction zones have generated basaltic magma in which Nb, and most other incompatible elements, are abundant and in which there is negligible depletion of HFSE relative to elements with similar compatibility. Reagan and Gill (1989) introduced the term “high-Nb basalt” to describe such rocks from the Costa Rican volcano Turrialba that contain 36ppm Nb which is not depleted relative to Light Rare Earth Elements (LREE), such as La, or Large Ion Lithophile Elements (LILE). For example, the value of (Nb/La)n, the Nb/La ratio normalised to the value for normal mid-ocean ridge basalt (N-MORB), is 0.91 in Turrialba high-Nb basalt, while values range from 0.33 to 0.42 in more typical arc-related magmatism from the same volcano. Sajona et al. (1994) subsequently used the term “Nb-enriched basalt” for basaltic rocks from Mindanao, the Philippines, containing 4-16ppm Nb and with (Nb/La)n ranging between 0.72 and 1.41.

Two main mechanisms have been proposed that might generate high-Nb basalt in these and other convergent margins. Reagan and Gill (1989) concluded that incompatible trace element enrichment is inherited from small-degree partial melts of an Ocean Island Basalt (OIB)-like source, which then interact with high-degree partial melts of depleted upper mantle. The OIB melts are undersaturated in rutile because they carry reduced C-O-H fluids and so Nb is not depleted relative to elements with similar compatibility. This contrasts with contemporaneous, presumed rutile-saturated, calc-alkaline magmatism at the same volcanic centres. Variations on this theme, with or without contributions from subducted crust and sediment, have been proposed for several locations (Storey et al., 1989; Leeman et al., 1990 and 2005; Richards et al., 1990; Petrone et al., 2003; Castillo et al., 2002 and 2007; Castillo, 2008; Petrone and Ferrari, 2008).

An alternative group of models arises from the observation that several high-Nb basalt suites occur in subduction zones where the subducting plate is young and, therefore, hot (Defant et al., 1992). Based on the premise that young subducted slabs are prone to melting (Defant and Drummond, 1990) and on the presence of putative slab melt magmatism in association with some high-Nb basalt occurrences, Defant et al. (1992) proposed that high-Nb basalt may be produced from mantle into which metasomatic, Nb-rich amphibole has been introduced by slab melt. This model has subsequently been applied to several high-Nb basalt occurrences (Sajona et al., 1994 and 1996; Kepezhinskas et al., 1995, 1996 and 1997; Escuder Viruete et al., 2007; Gómez-Tuena et al., 2007).

In this contribution we discuss the origin of Plio-Pleistocene high-Nb basalt magmatism from the Semporna peninsula of Sabah, Malaysia in northeastern Borneo. This site lies at the southern end of the Sulu Arc, an arcuate band of magmatism extending south-eastwards from the Zamboanga peninsula in western Mindanao through the Sulu Islands, such as Basilan and Jolo, towards NE Borneo (Fig. 1a). There is field and petrological evidence which suggests that the Sulu Arc produced subduction-related magmatism during the Miocene (Section 2.1). A deep trench (> 4800m) with high heat-flow lies to the north of the arc but Hamilton (1979) considered that this trench does not represent on-going subduction. There is little significant seismic activity currently associated with the Sulu Arc and tomographic imaging provides no evidence for a subducted slab beneath the islands (Spakman and Bijward, 1998; Rangin et al., 1999). Thus, although the term arc is appropriate to the bathymetry of the system it should not be used to infer that subduction is active, or that Plio-Pleistocene magmatism was caused by subduction-related processes.

We compare high-Nb magmatism from Sabah to magmatism in the rest of the Sulu Arc and to magmatic suites found elsewhere in SE Asia to investigate the nature of the mantle source and the lithosphere beneath Sabah. Then we discuss the implications of our findings for understanding mechanisms that might generate high-Nb basalt.

2. Setting and Samples

2.1 Mio-Pliocene Magmatism

Eurasia's eastern margin has interacted with the Pacific Plate throughout the Cenozoic generating a complex assemblage of plate fragments (Fig. 1a). The basement of Sabah was produced through accretion of Cretaceous ophiolitic fragments to the continental core of the island (Hall, 2002). From the Paleogene until the Early Miocene, southward-directed subduction of the proto-China Sea produced an accretionary margin in northern Borneo. The latter stages of this convergence occurred as the South China Sea Basin was opening to the north. K-Ar analyses obtained Middle to Late Miocene (12.9-9 Ma, Rangin et al., 1990; Bellon and Rangin, 1991) or Middle Miocene (18.8-14.4 Ma, Swauger et al., 1995) ages for Neogene magmatism in the Semporna and neighbouring Dent peninsulas, although these dates are uncertain because they were determined on whole rock samples that may have been subject to tropical weathering. The petrography and geochemistry of this magmatism is consistent with genesis in an island arc (Bellon & Rangin, 1991; Hutchison et al., 2000, Chiang, 2002) but the lack of tomographic evidence for dipping slabs, either modern or ancient (Spakman and Bijward, 1998; Rangin et al., 1999), has complicated efforts to determine the polarity of Neogene subduction. Hall (2002) used the geology of Sabah to infer that this subduction was directed towards the northwest. Chiang (2002) investigated this further by examining incompatible trace element ratios of Neogene arc magmatism throughout SE Sabah and also concluded that Celebes Sea crust was subducted beneath the Sulu Arc towards the northwest.

2.2 Plio-Pleistocene Magmatism

The youngest phase of magmatism in Sabah is the subject of this work. Plio-Pleistocene basalt and basaltic andesite lavas, cinder cones and occasional dykes are found at Tawau and Mostyn on the Semporna Peninsula (Fig. 1). At Tawau eruptions occurred through cinder cones while the Mostyn eruptions mainly occurred along N130°E-trending fissures. The ages of these rocks are poorly known. Lim and Hen (1985) suggested ages of 27 Ka or younger, while Rangin et al. (1990) obtained whole rock K-Ar dates of 2.8-3.1 Ma. However, Bellon and Rangin (1991) concede that the K-Ar data remain suspect, concluding that volcanism injected along the fissures is probably very young and that these faults are still active.

Plio-Pleistocene lavas from Tawau are aphyric to moderately (<20%) porphyritic basalts and basaltic andesites. Fresh plagioclase and olivine are the most abundant phenocryst phases in the basalts with magnetite and clinopyroxene occurring as minor phases in the groundmass. In the basaltic andesites, clinopyroxene is the most abundant phenocryst phase. Plagioclase is also the most abundant phenocryst phase in the Mostyn suite. Large, fresh phenocrysts of olivine are found in the most basic rocks and small orthopyroxene phenocrysts are the most common mafic phenocryst in more silicic rocks, although the total phenocryst content is particularly low in the latter. Clinopyroxene is a minor phase in the matrix of most Mostyn lavas.

3. Techniques

XRF analyses were performed using a Philips PW1480 XRF spectrometer at Royal Holloway, University of London. LOI was determined by heating the pre-dried sample at 1100°C for 20 minutes. Major element concentrations were analysed on fused discs of pre-dried sample mixed with pre-dried La_2O_3 Johnson-Mattey Spectroflux 105 (ratio sample:flux = 1:6). Trace element (Ni, Cr, V, Sc, Cu, Zn, Cl, Ga, Pb, Sr, Ba, Zr, Nb, Th, Y, La, Ce and Nd) concentrations were determined on pressed power pellets with matrix corrections based on major element compositions. Reproducibility (2sd of six replicate preparations) of XRF data is reported in Table 1; based on 25-35 international standards accuracy is comparable for major elements and for trace elements where these have been analysed by isotope dilution.

Sr and Nd isotopic analyses were conducted at the Arthur Holmes Isotope Geochemistry Laboratory at the University of Durham using a ThermoElectron Neptune multi-collector ICP-MS system. Details of the operating procedures and instrument configuration are given in Handley et al. (2007). Measured values for the NBS 987 and J&M standards ±2SD error during the same runs as the Semporna samples were 0.710270±18 (n=11) and 0.511101±5 (n=15), respectively. Data are reported relative to NBS 987 and J&M standard values of 0.71024 (Thirlwall, 1991) and 0.511110 (Royse et al., 1998), respectively. Total procedural blanks for Sr and Nd were determined by ICP-MS on a PerkinElmer ELAN 6000 quadrupole ICP-MS system at Durham University and were below 1.2 ng for Sr and 219 pg for Nd. These values are considered insignificant in relation to the quantity of Sr and Nd typically processed from Semporna rocks.

Pb isotope ratios were determined at the Scripps Institution of Oceanography following the procedure described in Janney and Castillo (1996; 1997). Rock powders were dissolved with a double-distilled, 2:1 mixture of concentrated $HF:HNO_3$ acid in Teflon beakers. Lead was separated from sample solutions using small ion exchange columns in an HBr medium and its isotopes were measured using a 9-collector, Micromass Sector 54 thermal ionization mass spectrometer. Lead isotopes were fractionation corrected using the isotope values of NBS 981 relative to those of Thirlwall (2000). Analytical uncertainties based on repeated measurements of standards are ± 0.008 for $^{206}Pb/^{204}Pb$ and $^{207}Pb/^{204}Pb$ and ± 0.030 for $^{208}Pb/^{204}Pb$. Routine analytical blank was generally <30 pg of Pb.

4. Results

Plio-Pleistocene lavas from Tawau and Mostyn display limited ranges of SiO_2 (49.44 to 56.56 wt.%) and MgO (4.36 to 7.66 wt.%). The Mostyn group are distinct from Tawau lavas in having lower K_2O and P_2O_5, and higher Fe_2O_3 and TiO_2 at any value of MgO (Fig. 2). For most major elements there is a significant amount of scatter at any MgO content. No correlations were found between major element concentrations and the modal abundance of any phenocryst phase. For the suite, as a whole, there is a general increase in SiO_2 with decreasing MgO, but most major elements show no simple variation with differentiation. This is also apparent for incompatible trace elements (Fig. 3). The Tawau lavas can be divided into four sub-groups (PP1 to PP4) for which, at any concentration of MgO, the concentrations of K_2O, P_2O_5, Sr, Nb, Rb and Ba all decrease in the order PP4 > PP3 > PP2 > Mostyn (Figs. 2 and 3). For Pb, Th, La, Ce and Nd a similar order exists but with PP2 lying between PP3 and PP4. The PP1 group has a very restricted range in MgO but frequently has incompatible element concentrations similar to, or lying on an extension of, the PP2 trend.

Concentrations of Ni (Fig. 3a) and Cr decrease with MgO as would be expected in magmas produced by differentiation of basaltic parents. In contrast, the majority of incompatible elements in the Tawau sub-groups and Mostyn lavas show behaviour that is not consistent with their expected compatibility in basaltic magma. The concentrations of these elements should increase as MgO falls but concentrations of K_2O, P_2O_5 and most other incompatible elements show relatively little variation or pronounced decreases with decreasing MgO (Figs. 2 and 3). This effect is particularly notable for P_2O_5 in the PP3 and Mostyn groups, which could indicate crystallisation of apatite, however, Semporna lavas are more mafic than would be suitable for apatite saturation at these P_2O_5 concentrations in basalt or alkali basalt (DeLong and Chatelain, 1990; Busà et al., 2002).

With respect to N-MORB, Semporna Plio-Pleistocene lavas contain high concentrations of the majority of incompatible elements (Fig. 4). As already noted, Tawau samples possess higher concentrations of most trace elements for any particular MgO content. The patterns for the most mafic rock from Tawau (SBK 13) and Mostyn have the smoothest patterns, in which HFSE display negligible depletion relative to neighbouring elements. This contrasts with typical subduction-related magmas, including Mio-Pliocene lavas from Tawau (Chiang, 2002). Negative relative Nb anomalies become increasingly apparent in more evolved rocks (Fig. 5). Concentrations of all LILE are elevated with respect to MORB. This is most apparent for Pb, which displays prominent positive anomalies compared to neighbouring elements in the MORB-normalised plot, but Pb is no more enriched than other LILE with respect to MORB (Fig. 4). Overall, the Semporna lavas possess higher concentrations of LILE and LREE than MORB and more closely resemble OIB than typical subduction-related magmatism, although LILE/LREE ratios are lower than in OIB. The most mafic Semporna lavas have HFSE/LILE and HFSE/LREE ratios comparable to or even higher than OIB.

Semporna Plio-Pleistocene lavas possess wide ranges in $^{87}Sr/^{86}Sr$ (0.704092 to 0.706291), $^{143}Nd/^{144}Nd$ (0.512846 to 0.512491) and Pb isotope ratios ($^{206}Pb/^{204}Pb$; 18.528 to 18.871, $^{207}Pb/^{204}Pb$; 15.566 to 15.667 and $^{208}Pb/^{204}Pb$; 38.598 to 39.116). Taking the Semporna lavas as a single suite the more evolved lavas tend to possess higher $^{87}Sr/^{86}Sr$ and Pb isotopic ratios and lower $^{143}Nd/^{144}Nd$. Despite the limited number of analyses this statement is also true for each site, with the Mostyn lavas offset to slightly higher $^{87}Sr/^{86}Sr$ and Pb, and lower $^{143}Nd/^{144}Nd$ at similar MgO (Fig. 6). Despite these offsets, co-variations between isotope ratios of different elements are particularly well defined for the suite as a whole. The most mafic lava has isotopic ratios that lie within the field of Indian Ocean MORB and that resemble values for several other small-volume volcanic provinces in SE Asia, but the more evolved lavas extend well beyond the field of Indian MORB (Fig. 7).

5. Discussion

The most mafic Semporna lava contains 7.66 wt.% MgO, which is close to the upper range of MgO contents in high-Nb basalts from other locations (8-9 wt.%), and is likely to provide a good estimate of the composition of parental magma. Although, SBK13 has a smooth trace element pattern (Fig. 4), mild to moderate Nb depletion $(Nb/K)_n < 1$ is apparent in many Semporna rocks, which might indicate a role for subduction-modified mantle. To understand the extent to which the relative Nb depletion of Semporna lavas is inherited from the mantle source it is necessary to determine how differentiation has affected trace elements.

5.1 Nb depletion of Semporna Plio-Pleistocene magma during differentiation

It is unlikely that the geochemical variations within the Semporna Plio-Pleistocene lavas result from fractional crystallisation of a uniform parental magma composition. First, concentrations of several elements that are usually incompatible during crystallisation of basaltic magma decrease with MgO. In all of the sub-groups P_2O_5, Nb and Sr decrease strongly from basalt to basaltic andesite. In the Mostyn group the other LILE and La also show the same effect (Fig. 3). Second, variations in Nb, K and La suggest unusual behaviour between HFSE, LILE and LREE. These elements have similar compatibilities in basaltic magma, therefore (Nb/La)n and (Nb/K)n should change little as basalt differentiates to basaltic andesite in a closed system. However, with the exception of relatively high Nb/La in two PP1 samples, both ratios become lower as MgO decreases (Fig. 5). Third, like Nb/La and Nb/K, the isotopic ratios of Sr, Nd and Pb should not vary in a suite of lavas produced by fractional crystallisation of uniform parental magma. In the Semporna lavas there are large ranges in each of these ratios, which change from the most to least evolved rocks (Fig. 6 and 7).

The strong inter-isotope correlations suggest that two main components are involved at Semporna (Fig. 7). Magma mixing, either between basic and evolved melts, or two mafic melts with different sources, is considered unlikely, since no petrographic evidence was found to indicate such a process. Therefore, we conclude that mafic, mantle-derived magma was contaminated by crust possessing high ^{87}Sr/^{86}Sr and Pb isotope ratios and low ^{143}Nd/^{144}Nd during differentiation from basalt to basaltic andesite. It is difficult to determine the nature of the contaminant because there are very few analyses of the compositions, and particularly isotopic ratios, of basement lithologies in Sabah. However, a number of reasonable inferences can be made. Mio-Pliocene arc magmatism from Sabah is characterised by Sr and Pb isotope ratios that are too low and by Nd isotope ratios that are too high to be the contaminant (Figs. 6). Similarly, the Mesozoic ophiolitic basement of Sabah, which is most likely to be comprised of fragments of oceanic crust resembling Indian Ocean MORB, would possess low ^{86}Sr/^{86}Sr and high ^{143}Nd/^{144}Nd (Omang and Barber, 1996; Weis and Frey, 1996).

In Sabah the only exposures of rocks derived from the lower crust are granite bodies. Mount Kinabalu, in north Sabah, is a composite granite that was intruded over a short period during the Miocene (Cottam et al., in press). Unfortunately, sufficient isotopic data do not exist to conduct detailed modelling of the effects of contamination by this material. However, the ^{86}Sr/^{86}Sr range, from 0.706364 to 0.707832 (Chiang, 2002), suggests that material of this type would not be a suitable contaminant. The lower end of the range would require more than 95% contamination of SBK13 to produce the highest ^{86}Sr/^{86}Sr in the Semporna suite while the upper end of the range would require 60% contamination. In both cases, such levels of contamination would produce magma that was more silicic than the most evolved basaltic andesite. Assimilation of such material can be examined further by using an analogous granitic body from the island of Palawan (Fig. 1). For reasonable values of r (the ratio of mass assimilated to mass crystallised), assimilation of Capoas granite during factional crystallisation of SBK13 fails to produce an array resembling the Semporna dataset (model LC 1 in Fig. 8). Bulk mixing of SBK13 with magma resembling the Capoas granite might achieve a closer fit to the isotopic and major element characteristics of the Semporna suite but would still require up to 40% contamination by the granitic component. As discussed above, there is no evidence of magma mixing in the Semporna rocks, which should be readily observed for such extensive contamination.

East Indonesian sediments (Vroon et al., 1995) may contain components that resemble the crustal fragments which were incorporated into SE Asian lithosphere. Therefore, we have also explored assimilation with fractional crystallisation (AFC) models using these sediments as crustal contaminants. Despite suitable Sr and Pb characteristics even the most extreme East Indonesia sediment composition does not possess sufficiently low $^{143}Nd/^{144}Nd$ to provide an appropriate contaminant (model EIS 1, Fig. 8). Increasing r, even to the relatively high value of 0.85, does not produce a fit to the data (model EIS 2) and reduces the amount of differentiation to the extent that there would virtually no change in major element chemistry of the magma.

Due to the restricted range of MgO contents in the Semporna lavas the contaminant requires very low $^{143}Nd/^{144}Nd$. Good fits to the Semporna dataset can be achieved for AFC models using assimilants with the isotopic characteristics of Archean crustal rocks via the moderate extents of crystallisation required to differentiate from basalt to basaltic andesite (models AC 1 and AC 2, Fig. 8). Although rocks of this age are not exposed in Sabah, Palaeoproterozoic ages have been determined for detrital zircons from the Crocker Formation in northern Borneo, for which van Hattum et al. (2006) postulated a local origin, and for inherited zircon crystals in the Kinabalu granite (Cottam et al., in press). Therefore, we postulate the Semporna crust contains Archean domains. Continental fragments may have been embedded in the Mesozoic oceanic lithosphere now forming the ophiolitic basement of Sabah, or may have been incorporated during northward and westward dispersion of continental material derived from the leading edge of the Australian continent as it interacted with SE Asia during the Cenozoic (Hutchison et al., 2001; Hall, 2002). van Leeuwen et al. (2007) recently proposed such an origin for the Malino complex, northwest Sulawesi, where Archean inherited zircons have been discovered.

5.2 Semporna parental magma without Nb depletion

Differentiation is the primary control on the extent of Nb depletion in Semporna lavas (Section 5.1). More specifically, Nb concentrations are lower and Nb-depletion, relative to other elements, is more marked in rocks that have experienced greater amounts of crustal contamination. The Nb contents of the most mafic basalts suggest that all magma left the mantle containing sufficient Nb to be classed as high Nb-basalt but during subsequent differentiation Nb, and several other elements, were diluted as many melt batches effectively evolved into Nb-enriched basalt (Fig. 3g). Therefore, classifying these rocks as high-Nb basalt or Nb-enriched basalt has no significance for source characteristics or processes; it is simply a function of the extent to which the melts differentiated.

Semporna lavas define single, coherent arrays when different isotopic ratios are compared with one another (Fig. 7) suggesting that there is only minor variation in the isotopic compositions of the mantle source and of the contaminant. These arrays are also consistent with a restricted range in Sr/Nd ratios in the parental magma. Like Nb/K and Nb/La (Fig. 5), many trace element ratios show less variation towards the more mafic end of the compositional range and converge on the values in SBK13. This suggests that differentiation was responsible for generating much of the heterogeneity in both isotopic ratios and incompatible element ratios between different members of the suite.

The most mafic lavas from Tawau and Mostyn display sub-parallel incompatible trace element patterns suggesting that their mantle sources did not possess relative depletion of Nb (Fig. 4). These patterns are very similar to those of parental magma in the rest of the Sulu Arc (Fig. 9a). The Sr, Nd and Pb isotope ratios of the least evolved northern, central and southern Sulu suites also converge on similar values suggesting shared sources. Castillo et al. (2007) demonstrated that northern and central Sulu Arc lavas possess isotopic ratios similar to those of basalts from the Scarborough Seamounts and Reed Bank in the South China Sea (Fig. 1a). This similarity extends to Quaternary magmatism from Hainan Island on the northern margin of the South China Sea (Figs. 7 and 9b). The three South China Sea suites possess inter-element ratios very similar to OIB. The Sulu Arc suites also show OIB-like patterns, with the exception of relative depletions in LREE, Sr and P (Fig. 9a).

5.3 Source of Semporna Plio-Pleistocene magmatism

Two main mechanisms have been proposed to explain how the mantle sources of high-Nb magmatism might develop. One involves metasomatism of mantle by partial melts from subducted crust (Defant et al., 1992) and, as such, implies an intrinsic role for subduction in producing such sources. The other advocates an enriched mantle resembling the source of OIB (Reagan and Gill, 1989), so is independent of subduction. Resolving which mechanism is responsible for producing high-Nb sources has important implications for understanding the dynamics of the subduction zones in which they occur.

5.3.1 Mantle metasomatism by partial melt from subducted basalt

Isotope ratios can be used to test whether partial melts derived from subducted lithosphere have metasomatised the Semporna mantle. Chiang (2002) examined variations in incompatible trace element ratios of Neogene magmatism across the Semporna and Dent peninsulas and concluded that the subducted slab was Celebes Sea oceanic lithosphere. Other studies have favoured the Sulu Sea as the source of the slab (e.g. Castillo et al., 2007) but the two basins are floored by basalt with similar isotopic compositions (Fig. 7) and so the distinction is irrelevant for the purpose of conducting this test. Isotopically distinctive basalt has been recovered from the Cagayan Ridge in the Sulu Sea, but the petrology and geochemistry of these rocks indicate that this bathymetric high originated as a volcanic arc (Bellon and Rangin, 1991; Spadea et al., 1991 and 1996). Features of this type have a lower probability of being subducted than the oceanic lithosphere of the adjacent basins. Therefore, the Cagayan Ridge samples are unlikely to represent a feasible slab melt composition.

If Semporna Plio-Pleistocene basalt originated in mantle that was metasomatised by partial melts from subducted lithosphere then (i) the most mafic Semporna lavas should possess isotope ratios closest to the compositions of Sulu or Celebes ocean floor basalt, and (ii) the Semporna isotopic arrays should trend towards that field. Some of the Semporna isotopic arrays do project back towards Sulu-Celebes compositions (e.g. $^{143}Nd/^{144}Nd$ versus $^{87}Sr/^{86}Sr$ and $^{208}Pb/^{204}Pb$ versus $^{206}Pb/^{204}Pb$). However, the $^{207}Pb/^{204}Pb$ versus $^{206}Pb/^{204}Pb$ and $^{143}Nd/^{144}Nd$ versus $^{207}Pb/^{204}Pb$ arrays clearly trend outside the range of Celebes and Sulu oceanic basalts and would infer a mantle with considerably higher $^{206}Pb/^{204}Pb$ at the measured $^{207}Pb/^{204}Pb$ or $^{143}Nd/^{144}Nd$ than the putative slab compositions (Fig. 7). Furthermore, the most mafic Semporna lava, which has experienced negligible contamination by crust (Section 5.1), lies significantly outside the Sulu-Celebes range for $^{87}Sr/^{86}Sr$, $^{206}Pb/^{204}Pb$ and $^{208}Pb/^{204}Pb$.

There is good evidence that subduction occurred beneath the Sulu Arc during the Miocene but the South China Sea sites lie as much as 1500km from Sulu and have not experienced recent subduction (Fig. 1a). It is extremely unlikely that metasomatism by partial melts of different subducted slabs at different times could yield sources with similar trace element and isotopic ratios beneath the Sulu Arc, Hainan Island, Scarborough Seamounts and Reed Bank (Figs. 7 and 9b). Therefore, we conclude that the source of Semporna Plio-Pleistocene lavas did not contain a significant contribution from partially-melted subducted lithosphere. Castillo et al. (2007) reached a similar conclusion for the central and northern Sulu Arc.

5.3.2 Intra-plate (OIB) mantle source

The least contaminated Semporna lava resembles many OIB in possessing high $^{87}Sr/^{86}Sr$ and Pb isotope ratios and low $^{143}Nd/^{144}Nd$ relative to the source of MORB (Fig. 7). Like magmatism in the South China Sea (Tu et al., 1991 and 1992; Flower et al., 1992), many incompatible trace element ratios of Semporna lavas also resemble OIB. Mafic Semporna lavas possess LILE/LILE, HSFE/HFSE and LILE/HFSE ratios similar to OIB, although concentrations of Sr are less enriched than other LILE. These traits are also shared by central and northern Sulu Arc lavas (Fig. 9a). The marked decrease of Sr with decreasing MgO in the Semporna suite suggests that this may be a product of crustal contamination such that SBK13 underestimates the true Sr content of the Semporna source, relative to other elements (Fig. 3c). Similarly, the decrease of P_2O_5 with MgO in most of the sub-groups (Fig. 2) means that the P content of the source may also be underestimated (Fig. 9a). All Sulu Arc lavas, however, have low LREE/HFSE and LREE/LILE, with respect to OIB. This is not a product of crustal contamination since the depletion of LREE relative to HFSE becomes less, not more, pronounced as MgO decreases (Fig. 5b). Indeed, (Nb/La)n is greater than 2 in the most mafic samples, suggesting a significant depletion of LREE with respect to the OIB source and to depleted mantle. Identifying a mechanism for producing LREE depletion of parental magma in the Sulu Arc would reconcile the differences between this and the South China Sea intra-plate magmatism (Fig. 9a) to a common OIB-like source.

The low LREE/HFSE and LREE/LILE ratios of mafic Sulu Arc magmatism might be produced in three ways: (1) through selective enrichment of LILE and HFSE in a source that was originally depleted in all incompatible elements, (2) during partial melting of an OIB source in the presence of a phase that retains LREE, or (3) through element fractionation as melt migrates through the mantle.

The source of Plio-Pleistocene Sulu Arc magmatism cannot be produced through enrichment of depleted mantle by a slab-derived fluid. This process would generate the marked HFSE depletions typical of subduction-related magmatism. Partial melts of subducted slabs are also precluded as an enriching agent on the basis of isotopic ratios (Section 5.3.1). Metasomatism of depleted mantle by small degree partial melts of the upper mantle can fractionate LILE, HFSE and REE relative to one another, with or without producing modal metasomatic phases (Bodinier et al., 1996; Pilet et al., 2004). This explanation might be feasible for the Sulu Arc alone but is more difficult to sustain in view of the many other similarities between Sulu Arc and South China Sea lavas (Fig. 7 and 9b). A distinct LREE-enrichment event might have affected the South China Sea mantle, independent of an LILE- and HFSE-enrichment affecting the Sulu Arc and South China Sea. This, however, would require an entirely complementary relationship in the chemical budgets of the two metasomatic agents such that their summed effect produced a South China Sea mantle source with OIB-like chemistry. We consider this highly unlikely. Therefore, we conclude that enrichment of depleted mantle, alone, cannot have produced the similar sources of the Sulu Arc and South China Sea magmatic suites.

A wide range of minor, metasomatic phases might be present in the source of OIB-like magmas that could fractionate trace elements, particularly at low degree of partial melting. It is not possible to constrain possible roles for all of these but several obvious possibilities can be eliminated. Phlogopite and kaersutite can produce significant fractionation of HFSE from LREE but this should be in the opposite sense to that required to generate high Nb/La in Sulu i.e. Nb would be retained in the source relative to LREE yielding low-Nb/La melt (Schmidt et al., 1999; Tiepolo et al., 2000). This partitioning has strong compositional-dependence in amphibole but the ratio of partition coefficients approaches unity as the host rock Mg# approaches mantle values and does not reverse (Tiepolo et al., 2000). Apatite would preferentially retain LREE as well as P, which is mildly depleted in the Semporna rocks, but would also be expected to generate a significant negative Th anomaly (Chazot et al., 1996), which is not observed (Fig. 9a). Although other minor phases may be able to partition elements in a suitable way, the absolute concentration of incompatible elements in the different magmatic suites is inconsistent with derivation by variable degrees of partial melting of similar sources. The imprint of distinctive minor phases should be more apparent in low degree partial melts. With increasing degrees of partial melting the residue would evolve towards a simpler assemblage with partition coefficients resembling those typical of the upper mantle and yield magma with lower concentrations of all incompatible elements. However, HFSE/LREE fractionation, with respect to OIB, is absent in South China Sea lavas, which possess the high incompatible element concentrations expected of lower degrees of partial melting (Fig. 9a). High Nb/La is found in the Sulu Arc lavas that have lower concentrations of incompatible elements. Therefore, we consider it unlikely that the LREE depletion of Sulu Arc magmatism results from low-degree partial melting of OIB source mantle in the presence of a residual phase with high D_{LREE}.

Interaction between melt and mantle peridotite may seem an unlikely process to produce the observed fractionation of LREE from LILE and HFSE, given that element partitioning should be governed by similar distribution coefficients to those operating during partial melting (Navon and Stolper, 1987). Indeed, experimental studies have concluded that reaction with peridotite will decrease the concentrations of HFSE in melt, relative to other incompatible elements (Kelemen et al., 1990 and 1993). Despite this, empirical evidence suggests that REE can be fractionated from other incompatible elements as basaltic melt interacts with upper mantle. Refertilization of depleted mantle by basaltic magma has been proposed as the origin of layered websterites (‘group C’ pyroxenites) from the “asthenospherised” part of the Ronda massif in Spain (Lenoir et al., 2001; Bodinier et al., 2008). Both the websterite layers and their host peridotites in the sub-lithospheric domain show strong enrichment of LREE relative to HSFE and LILE, while LILE/HFSE ratios display much less fractionation (Bodinier et al., 2008). A complementary (melt) product, with high HFSE/LREE and LILE/LREE ratios, is not observed at Ronda but the massif provides evidence that melt-mantle interaction can modify LREE concentrations of magma relative to elements with similar distribution coefficients.

5.3.3 A model for intra-plate magmatism in the Sulu Arc and South China Sea

Intra-plate magmatism in the Sulu Arc and South China Sea was derived from an OIB-like source. South China Sea magmatism occurred where the lithosphere was experiencing, or had recently experienced, mechanical thinning. Hainan, where most lava was erupted into the Lei-Qiong graben, was extended by pull-apart tectonics on the northern margin of the South China Sea (Tu et al., 1991; Flower et al., 1992). Reed Bank lies on edge of a presumed continental fragment on the conjugate, southern, extended margin of the inactive South China Sea. The mid- to late-Neogene Scarborough Seamounts were generated close to the South China Sea spreading axis, which had become extinct 5-10 million years previously (Fig. 1a; Tu et al., 1992). The continental margin settings of Hainan and Reed Bank could be consistent with sources in the mantle lithosphere. However, the South China Sea lithosphere was very young when intra-plate magmatism occurred. Therefore, even if the source of this suite was hosted in the lithosphere it can have resided there for only a very short period since accretion/addition from the convecting mantle. In view of the widespread distribution of magmatic suites with similar trace element and isotopic chemistry (Fig. 9), we conclude that the source of intra-plate magmatism in the South China Sea and its extended margins was an OIB-like component in the upper mantle that melted as it upwelled beneath recently thinned lithosphere. As well as reducing the thickness of lithospheric mantle, preceding extension could provide large, lithosphere-penetrating structures that would facilitate transport of melt towards the surface and, thus, reduce the opportunity for interaction with the lithospheric mantle or crust.

Plio-Pleistocene magmatism in the Sulu Arc was extracted from similar enriched mantle, also during upwelling beneath thinned lithosphere. Upwelling might have occurred beneath localised sites of extension, but the Sulu Arc lithosphere would have experienced substantial thinning during Miocene subduction in the Sulu Arc (Andrews and Sleep, 1974; Hamilton, 1995; Macpherson and Hall, 2002; Arcay et al., 2006). Such thinning is probably less reliant on mechanical deformation than is the case for extended margins. Instead, rheological changes result in (i) convective erosion, or corner flow, removing mass from the base of arc lithosphere (Hamilton, 1995; Billen and Gurnis, 2001; Arcay et al., 2006; Macpherson, 2008) and/or (ii) gravitational instabilities removing dense material from throughout the thickness of arc lithosphere (Rudnick, 1995). Lithospheric thin-spots produced by Miocene subduction would provide sites where enriched mantle could upwell and produce small volumes of intra-plate magmatism along the axis of the former arc front. In contrast to locations in and around the South China Sea, large, lithosphere-penetrating, extensional structures would be rare in the Sulu environment, increasing the probability that melt would interact with lithospheric mantle during transport from the subjacent asthenosphere.

Semporna lies at the end of the northeast-southwest trending Sulu Arc (Fig. 1a). Further southwest are several other Plio-Pleistocene to Recent low-volume volcanic fields that cap the topography of central Borneo at Hose Mountains, Kelian, Metalung, Nuit and Usun Apau (Fig. 1a). There are very few studies of these occurrences but data from Chiang (2002) show that basalt from Kelian possesses c. 20ppm Nb and there is a distinct decrease in Nb/K with

MgO, similar to that seen in the Sulu Arc (Fig. 5a). Therefore, the same enrichment responsible for Sulu Arc and South China Sea magmatism may be present in upper mantle beneath Borneo and has encountered thin spots in the lithosphere that have allowed it to upwell and melt. To the north of Borneo young, high-Nb magmatism from northern Palawan (Fig. 1a) may also share the same source (Arcilla et al., 2003).

5.4 Implications for high-Nb magmatism in active arcs

Our findings indicate that high-Nb basaltic magmatism in the Semporna peninsula, and elsewhere in the Sulu Arc, does not require a contribution from subducted crust. If this conclusion is also valid in arcs where high-Nb magmatism is contemporaneous with typical arc magmatism then parts of the mantle wedge must escape significant metasomatism by material derived from the subducted slab. In particular, the original finding of Reagan and Gill (1989); that high-Nb basalts and calc-alkaline magma were erupted from the same centre, implies that slab-fluxed and un-fluxed mantle may be present within the source volume of a single volcano.

Intra-plate or OIB-type mantle has been advocated as the prevalent mantle wedge component in some volcanic arcs (e.g. Mexico, Gómez-Tuena et al., 2007). In view of the low recycled flux inferred for Semporna mantle it is tempting to regard the source of Plio-Pleistocene magmatism as representative of the bulk mantle beneath the Sulu Arc. However, the relatively low volumes of Semporna Plio-Pleistocene magmatism indicate a finite source that was rapidly exhausted after melting commenced. This conclusion is reinforced by the other sites in Borneo and the South China Sea, where OIB-like magma also occurs in low volumes. Such enriched domains may be relatively common in the upper mantle beneath much of SE Asia, but their signature would be swamped when conditions allow partial melting of the more refractory mantle in which the enrichments are hosted. This is analogous to the recognition of melt derived from enriched mantle on the margins of active rift systems. Such domains may also be present beneath the rift but their signature is overwhelmed where partial melting becomes more extensive close to rift axes (e.g. Iceland, Fitton et al., 2003).

5.5 The high-Nb basalt – adakite association

The frequent association of high-Nb basalt with adakitic magmatism led Defant et al. (1992) to postulate a genetic link, in which adakitic magma metasomatised the mantle to produce the high-Nb source. Defant and Drummond (1990) regarded adakites as direct samples of magma generated by partial melting of subducted basaltic crust but an increasing number of studies have questioned this model (Garrison and Davidson, 2003; Prouteau and Scaillet, 2003; Chiaradia et al., 2004; Macpherson et al., 2006; Eiler et al., 2007; Rodriguez et al., 2007). The sources of high-Nb basalt in Semporna, and related SE Asian sites, cannot have been produced by metasomatism of depleted mantle by slab melt (Section 5.3.1). Furthermore, although adakitic rocks have been found in the northern Sulu Arc (Sajona et al. 1996; Castillo et al., 2007) there is no evidence for adakitic magmatism in the Semporna peninsula. Similarly, adakitic magmatism has not been documented in association with the high-Nb basalt suites of the South China Sea and its margins. Therefore, Semporna and the South China Sea weaken the case for a petrogenetic link where these two distinctive “flavours” of magmatism occur in a single subduction zone.

Despite this assertion, the fact remains that several margins have produced both adakitic and high-Nb magmatism (Defant et al., 1992). Macpherson et al. (2006) used an example from the East Philippine Arc to show that adakitic magmatism can occur where hydrous arc basalt, produced by fluid-fluxed melting of the mantle wedge, ponds at relatively deep levels and crystallises garnet (± amphibole). Adakitic magma was produced when this crystal assemblage was removed from hydrous basaltic magma or when the resulting cumulate rocks experienced partial melting. The East Philippine setting was conducive to these processes because the plate margin was young and so the arc lithosphere had experienced limited thinning. The deeper parts of this thick arc lithosphere acted as a barrier to melt transport promoting crystallisation of basalt at depth. Meanwhile, the shallow portions had yet to develop substantial magma plumbing systems, therefore, geochemical evidence of deep differentiation was not overprinted by subsequent differentiation when the adakitic melt was emplaced (Macpherson, 2008).

The potential for an active arc to generate high-Nb magmatism depends on the presence of a suitably enriched source in the mantle wedge. But, like adakitic magma, the distinctive geochemistry of high-Nb basalt is most likely to be preserved where it is not overprinted by interaction with large volumes of melt derived from slab-modified mantle wedge and/or by differentiation in the shallow crust. We propose that the occurrence of adakitic and high-Nb magmatism together in an arc does not reflect a genetic link between their sources. Instead, we postulate that there is a significant increase in the probability that magmatism will retain distinctive geochemical signatures derived at depth e.g. either by deep differentiation (adakitic magmatism) or inherited from a distinctive mantle source (high-Nb magmatism), during transport through arc lithosphere that receives a low flux of melt from slab-modified mantle and/or hosts poorly developed magma plumbing in the shallow crust.

6. Conclusions

1. Plio-Pleistocene basalts and basaltic andesites from the Semporna peninsula of the southern Sulu Arc contain higher concentrations of Nb than typical arc magmatism. The most mafic lavas have negligible Nb depletions relative to elements with similar compatibility. Depletion of Nb, and several other incompatible elements, occurred during differentiation from basalt to basaltic andesite. This was accompanied by striking changes in isotopic ratios that indicate interaction with the crust. The isotopic characteristics of the contaminant indicate an ancient, possibly Archean, component is present in the Sabah crust.

2. The primitive Semporna lavas closely resemble high-Nb and Nb-enriched basalts from the central (Sulu Islands) and northern (Zamboanga) segments of the Sulu Arc. Isotopic ratios preclude a role for metasomatism of Sulu Arc mantle by melt derived from subducted Sulu Sea or Celebes Sea oceanic crust. Mafic Sulu Arc lavas possess incompatible trace element ratios that resemble ocean island basalt but are depleted in light rare earth elements. Sulu Arc basalts also resemble mafic magmatism at several sites in and around the South China Sea, which differ only in lacking light rare earth element depletion. This similarity and the range of localities indicates a common source present in the convecting upper mantle. This magmatic province may also extend southwest into central Borneo.

3. The Sulu Arc runs from the Zamboanga peninsula through the Sulu Islands to the Semporna peninsula, yet there is little other geological or geophysical evidence to support active subduction beneath this structure. Plio-Pleistocene magmatism resulted from upwelling of OIB-like domains in the upper mantle into lithospheric thin spots that were produced during Miocene subduction.

4. Light rare earth element depletion of Sulu magmatism cannot be attributed to crustal contamination and probably occurred when basaltic melt interacted with mantle peridotite during transport through the Sulu Arc lithosphere. South China Sea magmatism may have escaped this process due to transport along extensional structures in oceanic lithosphere and stretched continental margins.

Acknowledgements

The SE Asia Research Group, Royal Holloway University of London, funded much of this work. We are grateful to Jon Davidson and James Gill for discussion. Matthew Leybourne, an anonymous reviewer and, editor, Richard Wysoczanski are thanked for their constructive comments upon the manuscript.

References

Andrews, D.J., Sleep, N.H., 1974. Numerical modelling of tectonic flow behind island arcs. Geophysical Journal of the Royal Astronomical Society 38, 237-251.

Arcay, D., Doin, M.-P., Tric, E., Bousquet, R., de Capitani, C., 2006, Overriding plate thinning in subduction zones: Localized convection induced by slab dehydration. Geochemistry, Geophysics, Geosystems 7, Q02007, doi: 10.1029/2005GC001061.

Arcilla, C., Maximo, R., Vogel, T., Patino, L., Flower, M., Mukasa, S., 2003. High-Nb lavas from northern Palawan: implications for high field strength enrichment in southern Philippine Arc. Geophysical Research Abstracts 5, 03451.

Bellon, H., Rangin, C., 1991. Geochemistry and isotopic dating of the Cenozoic volcanic arc sequences around the Celebes and Sulu Seas. In: Silver, E.A., Rangin, C. & von Breymann, M.T. (Eds.), Proceedings of the Ocean Drilling Program Scientific Results 124, 321-338.

Billen, M.I., Gurnis, M., 2001. A low viscosity wedge in subduction zones. Earth and Planetary Science Letters 193, 227-236.

Bodinier, J.-L., Merlet, C., Bedini, R.M., Simien, F., Remaidi, M., Garrido, C.J., 1996. Distribution of niobium, tantalum, and other highly incompatible elements in the lithospheric mantle: The spinel paradox. Geochimica et Cosmochimica Acta 60, 545-550.

Bodinier, J.-L., Garrido, C.J., Chanefo, I., Brugier, O., Gervilla, F., 2008. Origin of pyroxenite-peridotite veined mantle by refertilization reactions: Evidence from the Ronda peridotite (southern Spain). Journal of Petrology 49, 999-1025.

Busà, T., Clochiatti, R., Cristofolini, R., 2002. The role of apatite fractionation and REE distribution in alkaline rocks from Mt. Etna, Scicily. Mineralogy and Petrology 74, 95-114.

Castillo, P.R., 2008. Origin of the adakite – high-Nb basalt association and its implications for postsubduction magmatism in Baja California, Mexico. Geological Society of America Bulletin 120, 451-462. doi:10.1130/B26166.1.

Castillo, P.R., Solidum, R.U., Punogbayan, R.S., 2002. Origin of high field strength element enrichment in the Sulu Arc, southern Philippines, revisited. Geology 30, 707-710.

Castillo, P.R., Rigby, S.J., Solidum, R.U., 2007. Origin of high field strength element enrichment in volcanic arcs: geochemical evidence from the southern Sulu Arc, southern Philippines. Lithos 97, 271-288. doi: 10.1016/j.lithos.2006.12.012.

Chazot, G., Menzies, M.A., Harte, B., 1996. Determination of partition coefficients between apatite, clinopyroxene, amphibole, and melt in natural spinel lherzolites from Yemen: Implications for wet melting of the lithospheric mantle. Geochimica et Cosmochimica Acta 60, 423-437.

Chiang, K.K., 2002. Geochemistry of the Cenozoic igneous rocks of Borneo and tectonic implications. Unpublished PhD Thesis, University of London, 364pp.

Chiaradia, M., Fontbote, L., Beate, B., 2004. Cenozoic continental arc magmatism and associated mineralization in Ecuador. Mineralium Deposita 39, 204–222. doi: 10.1007/s00126–003–0397–5.

Cottam, M., Hall., R., Sperber, C., Armstrong, R., in press. Pulsed emplacement of a layered granite: New high-precision age data from Mount Kinabalu, North Borneo. Journal of the Geological Society of London.

Defant, M.J., Drummond, M.S., 1990. Derivation of some modern arc magmas by melting of young subducted lithosphere. Nature 347, 662-665.

Defant, M.J., Jackson, T.E., Drummond, M.S., De Boer, J.Z., Bellon, H., Feignson, M.D., Maury, R.C., Stewart, R.H., 1992. The geochemistry of young volcanism throughout western Panama and southeastern Costa Rica: an overview. Journal of the Geological Society of London 149, 569-579.

DeLong, S.E. and Chatelain, C., 1990. Trace-element constraints on accessory-phase saturation in evolved MORB magma. Earth and Planetary Science Letters 101, 206-215.

DePaolo, D.J., 1981. Trace element and isotopic effects of combined wallrock assimilation and fractional crystallisation. Earth and Planetary Science Letters 53, 189-202.

Eiler, J.M., Schiano, P., Valley, J.W., Kita, N.T., Stolper, E.M., 2007. Oxygen-isotope and trace element constraints on the origins of silica-rich melts in the mantle. Geochemistry, Geophysics, Geosystems 8, Q09012. doi: 10.1029/2006GC001503.

Encarnación, J., Mukasa, S.B., 1997. Age and geochemistry of an ‘anorogenic’ crustal melt and implications for I-type granite petrogenesis. Lithos 42, 1-13.

Escuder Viruete, J., Contreras, F., Stein, G., Urien, P., Joubert, M., Perez-Estaun, A., Friedman, R., Ullrich, T., 2007. Magmatic relationships and ages between adakites, magnesian andesites and Nb-enriched basalts from Hispanola: Record of a major change in Carribean island arc sources. Lithos 99, 151-177. doi:10.1016/j.lithos.2007.01.008.

Fitton J. G., Saunders, A.D., Kempton, P.D., Hardarson, B.S., 2003. Does depleted mantle form an intrinsic part of the Iceland plume? Geochemistry, Geophysics, Geosystems 4, 1032. doi:10.1029/2002GC000424.

Flower, M.J.F., Zhang, M., Chen, C.-Y., Tu, K., Xie, G., 1992. Magmatism in the South China Sea Basin 2. Post-spreading Quaternary basalts from Hainan Island, south China. Chemical Geology 97, 65-87.

Garrison, J.M., Davidson, J.P., 2003. Dubious case for slab melting in the Northern volcanic zone of the Andes. Geology 31, 565-568.

Gómez-Tuena, A., Langmuir, C.H., Goldstein, S.L., Straub, S.M., Ortega-Gutiérrez, F., 2007. Geochemical evidence for slab melting in the Trans-Mexican Volcanic Belt. Journal of Petrology 48, 537-562. doi:10.1093/petrology/eg1071.

Hall, R., 2002. Cenozoic geological and plate tectonic evolution of SE Asia and the SW Pacific: computer-based reconstructions, model and animations. Journal of Asian Earth Sciences 20, 353-434.

Haile, N.S., Wong, N.P.Y., Nuttall, C. P., 1965. The geology and mineral resources of the Dent Peninsula, Sabah. British Borneo Geological Survey Memoir 16, 199pp.

Hamilton, W.B., 1979. Tectonics of the Indonesian Region. US Geological Survey Professional Paper 1078, 345pp.

Hamilton, W.B., 1995. Subduction systems and magmatism. In: Smellie, J.L. (Eds.) Volcanism associated with extension at consuming plate margins. Geological Society of London Special Publication 81, 3-28.

Handley, H.K., Macpherson C.G., Davidson, J.P., Berlo, K., Lowry, D., 2007. Constraining fluid and sediment contributions to subduction-related magmatism in Indonesia: Ijen Volcanic Complex. Journal of Petrology 48, 1155-1183. doi:10.1093/petrology/egm013.

Hart, S.R., 1984. A large-scale isotope anomaly in the Southern Hemisphere mantle. Nature 309, 753-757.

Hutchison, C.S., Bergman, S.C., Swauger, D.A., Graves, J.E., 2000. A Miocene collisional belt in north Borneo: uplift mechanism and isotatic adjustment quantified by thermochronology. Journal of the Geological Society of London 157, 783-793.

Hutchison, C.S., Bergman, S.C., Swauger, D.A., Graves, J.E., 2001. Discussion of a Miocene collisional belt in north Borneo: uplift mechanism and isotatic adjustment quantified by thermochronology. Journal of the Geological Society of London 158, 398-400.

Jacobsen, S.B., Wasserburg, G.J., 1978. Interpretation of Nd, Sr and Pb isotope data from Archean migmatites in Lofoten-Verterålen, Norway. Earth and Planetary Science Letters 41, 245-253.

Janney, P.E., Castillo, P.R., 1996. Basalts from the Central Pacific Basin: evidence for the origin of Cretaceous igneous complexes in the Jurassic Western Pacific. Journal of Geophysical Research 101, 2875-2894.

Janney, P.E., Castillo, P.R., 1997. Geochemistry of Mesozoic Pacific MORB: Constraints on melt generation and the evolution of the Pacific upper mantle. Journal of Geophysical Research 102, 5207-5229.

Kelemen, P.B., Shimizu, N., Dunn, T., 1990. Relative depletion of niobium in some arc magmas and the continental crust: partitioning of K, Nb, La and Ce during melt/rock interaction in the upper mantle. Earth and Planetary Science Letters 120, 111-134.

Kelemen, P.B., Johnson, K.T.M., Kinzler, R.J., Irving, A.J., 1993. High-field-strength element depletion in arc basalts due to mantle-melt interaction. Nature 345, 521-524.

Kepezhinskas, P.K., Defant, M.J., Drummond, M.S., 1995. Na metasomatism in the island-arc mantle by slab melt – peridotite interaction: evidence from mantle xenoliths in the north Kamchatka arc. Journal of Petrology 36, 1505-1527.

Kepezhinskas, P.K., Defant, M.J., Drummond, M.S., 1996. Progressive enrichment of island-arc mantle by melt-peridotite interaction from Kamchatka adakites. Geochimica et Cosmochimica Acta 60, 1217-1229.

Kepezhinskas, P.K., McDermott, F., Defant, M.J., Hochstaedter, A., Drummond, M.S., Hawkesworth, C.J., Kolokov, A., Maury, R.C., Bellon, H., 1997. Trace element and Sr-Nd-Pb isotopic constraints on a three-component model of Kamchatka arc petrogenesis. Geochimica et Cosmochimica Acta 61, 577-600.

Kirk, H.J.C., 1962. The geology and mineral resources of the Semporna Peninsula, North Borneo. Geological Survey Malaysia, Sabah, 178pp.

Lee, D.T.C., 1988. Gunung Pock Area, Semporna Peninsula, Sabah, Malaysia: Explanation of sheet 4/118/10. Geological Survey of Malaysia, Sabah, 120pp.

Leeman, W.P., Smith, D.R., Hildreth, W., Palacz, Z., Rogers, N., 1990. Compositional diversity of late Cenozoic basalts in a transect across the southern Washington Cascades: Implications for subduction zone magmatism. Journal of Geophysical Research 95, 19561-19582.

Leeman, W.P., Lewis, J.F., Evarts, R.C., Conrey, R.M., Streck, M.J., 2005. Petrologic constraints on the thermal structure of the Cascades arc. Journal of Volcanology and Geothermal Research 140, 67-105. doi:10.1016/j.jvolgeores.2004.07.016.

Lenoir, X., Garrido, C.J., Bodinier, J.-L., Dautria, J.-M., Gervilla, F., 2001. The recrystallisation front of the Ronda peridotite: Evidence for melting and thermal erosion of subcontinental lithospheric mantle beneath the Alboran Basin. Journal of Petrology 42, 141-158.

Leong, K.M., 1974. The geology and mineral resources of the Darvel Bay and Upper Segama Area, Sabah. Malaysia Geological Survey Borneo Region, 4, 354pp.

Lim, P.S., 1981. Wullersdorf Area, Sabah, Malaysia. Geological Survey of Malaysia, Sabah Report, 15, 105 pp.

Lim, P.S., Heng, Y.E., 1985. Geological map of Sabah 1:500,000. Geological Survey of Malaysia.

Macpherson, C.G., 2008. Lithosphere erosion and crustal growth in subduction zones: Insights from initiation of the nascent East Philippine Arc. Geology 36, 311-314.

Macpherson, C.G., Hall, R., 2002. Timing and tectonic controls in the evolving orogen of SE Asia and the western Pacific and some implications for ore generation. In: Blundell, D.J., Neubauer, F. & von Quant, A (Eds.) The Timing and Location of Major Ore Deposits in an evolving Orogen. Geological Society of London Special Publication 204, 49-67.

Macpherson, C.G., Dreher, S.T., Thirlwall, M.F., 2006. Adakites without slab melting: high pressure processing of basaltic island arc magma, Mindanao, the Philippines. Earth and Planetary Science Letters 243, 581–593. doi: 10.1016/j.epsl.2005.12.034.

Navon, O., Stolper, E., 1987. Geochemical consequences of melt percolation: The upper mantle as a chromatographic column. Journal of Geology 95, 285-307.

Omang, S.A.K., Barber, A.J., 1996. Origin and tectonic significance of the metamorphic rocks associated with the Darvel Bay ophiolite, Sabah, Malaysia. In: Hall, R., Blundell, D. (Eds.) Tectonic Evolution of Southeast Asia, Geological Society of London Special Publication 106, 263-270.

Petrone, C.M., Francalanci, L., Carlson, R.W., Ferrari, L., Conticelli, S., 2003. Unusual coexistence of subduction-related and intraplate-type magmatism: Sr, Nd and Pb isotope and trace element data from the magmatism of the San Pedro – Ceboruco graben (Nayarit, Mexico). Chemical Geology 192, 1-24.

Petrone, C.M., Ferrari, L., 2008. Quaternary adakite – Nb-enriched basalt association in the western Trans-Mexican Volcanic Belt: is there any slab melt evidence? Contributions to Mineralogy and Petrology 156, 73-86. doi: 10.1007/s00410-007-0274-9.

Pilet, S., Hernandez, J., Bussy, F., Sylvester, P.J., 2004. Short-term metasomatic controls on the Nb/Th ratios in the mantle sources of intraplate basalt. Geology 32, 113-116. doi: 10.1130/G19953.1.

Prouteau, G., Scaillet, B., 2003. Experimental constraints on the origin of the 1991 Pinatubo dacite. Journal of Petrology 44, 2203–2241. doi: 10.1093/petrology/egg075.

Rangin, C., Bellon, H., Benard, F., Letouzey, J., Müller, C., Tahir, S., 1990. Neogene arc-continent collision in Sabah, N. Borneo (Malaysia). Tectonophysics 183, 305-319.

Rangin, C., Spackman, W., Pubellier, M., Bijwaard, H., 1999. Tomographic and geological constraints on subduction along the eastern Sundaland continental margin (South-east Asia). Bulletin de la Société Géologique de France 170, 775-788.

Reagan, M.K., Gill, J.B., 1989. Coexisting calk-alkaline and high-niobium basalt from Turrialba volcano, Costa Rica: implications for residual titanites in arc magma series. Journal of Geophysical Research 94, 4619-4633.

Richards, J.P., Chappell, B.W., McCulloch, M.T., 1990. Intraplate-type magmatism in a continent-island-arc collision zone: Porgera intrusive complex, Papua New Guinea. Geology 18, 958-961.

Rodriguez, C., Selles, D., Dungan, M., Langmuir, C., Leeman, W., 2007. Adakitic dacites formed by intracrustal crystal fractionation of water rich parent magmas at Nevado de Longavi volcano (36.2°S; Andean Southern volcanic zone, Central Chile). Journal of Petrology 48, 2033–2061. doi: 10.1093/petrology/egm049.

Royse, K., Kempton, P.D., Darbyshire, D.P.F., 1998. Procedure for the analysis for rubidium-strontium and samarium-neodymium isotopes at the NERC Isotope Geosciences Laboratory. NERC Isotope Geosciences Laboratory Report Series 121.

Rudnick, R.L., 1995. Making continental crust. Nature 378, 571-578.

Schmidt, K.H., Bottazzi, P., Vannucci, R., Mengel, K., 1999. Trace element partitioning between phlogopite, clinopyroxene and leucite lamproite melt. Earth and Planetary Science Letters 168, 287-299.

Sajona, F.G., Bellon, H., Maury, R.C., Pubellier, M., Cotton, J., Rangin, C., 1994. Magmatic response to abrupt changes in tectonic setting: Pliocene-Quaternary calc-alkaline lavas and Nb-enriched basalts of Leyte and Mindanao (Philippines). Tectonophysics 237, 47-72.

Sajona, F.G., Maury, R.C., Bellon, H., Cotton, J., Defant, M., 1996. High field strength element enrichment of Pliocene-Pleistocene island arc basalts, Zamboanga peninsula, western Mindanao (Philippines). Journal of Petrology 37, 693-726.

Spadea, P., Beccaluva, L., Civetta, L., Coltorti, M., Dostal, J., Sajona, F., Serri, G., Vaccaro, C., Zeda, O., 1991. Petrology of basic igneous rocks from the floor of the Sulu Sea. : Silver, E.A., Rangin, C., von Breymann, M.T. (Eds.), Proceedings of the Ocean Drilling Program Scientific Results, 124, 251-269.

Spadea, P., D'Antonio, M., Thirlwall, M., 1996. Source characteristics of the basement rocks from the Sulu and Celebes Basins (Western Pacific): chemical and isotopic evidence. Contributions to Mineralogy and Petrology 123, 159-176.

Spakman, W., Bijwaard, H., 1998. Mantle structure and large-scale dynamics of South-East Asia. In: Wilson, P., Michel, G. W. (Eds.), The Geodynamics of S and SE Asia (GEODYSSEA) Project. GeoForschingsZentrum, Potsdam, Germany, 313-339.

Storey, M., Rogers, G., Saunders, A.D., Terrell, D.J., 1989. San Quintin volcanic field, Baja California, Mexico: within-plate magmatism following ridge subduction. Terra Nova 1, 195-202.

Sun, S.–S., McDonough, W.F., 1989. Chemical and isotopic systematics of oceanic basalts: implications for mantle composition and processes. In: Saunders, A. D., Norry, M.J. (Eds.) Magmatism in the Ocean Basins, Geological Society of London Special Publication 42, 313-345.

Swauger, D.A., Bergman, S.C., Graves, J.E., Hutchison, C.S., Surat, T., Morillo, A.P., Benavidez, J.J., Pagado, E.S., 1995. Tertiary stratigrapic, tectonic, and thermal history of Sabah, Malaysia: results of a 10 day reconnaissance field study and laboratory analyses. ARCO International Oil and Gas Co. unpublished report TRS 95-0036.

Thirlwall, M.F., 1991. Long-term reproducibility of multicollector Sr and Nd isotope ratio analysis. Chemical Geology (Isotope Geoscience Section) 94, 85-104.

Thirlwall, M.F., 2000. Inter-laboratory and other errors in Pb isotope analyses investigated using a ^{207}Pb-^{204}Pb double spike. Chemical Geology 163, 299-322.

Thirlwall, M.F., Smith, T.E., Graham, A.M., Theodorou, N., Hollings, P., Davidson, J.P., Arculus, R.J., 1994. High field strength element anomalies in arc lavas: Source or process. Journal of Petrology 35, 819-838.

Tiepolo, M., Vannucci, R., Oberti, R., Foley, S., Bottazzi, P., Zanetti, A., 2000. Nb and Ta incorporation and fractionation in titanian pargasite and kaersutite: crystal-chemical constraints and implications for natural systems. Earth and Planetary Science Letters 176, 185-201.

Tu, K., Flower, M.F.J., Carlson, R.W., Zhang, M., Xie, G., 1991. Sr, Nd, and Pb isotopic compositions of Hainan basalts (south China): Implications for a subcontinental lithosphere Dupal source. Geology 19, 567-569.

Tu, K., Flower, M.F.J., Carlson, R.W., Xie, G., Chen, C.-Y., Zhang, M., 1992. Magmatism in the South China Basin 1. Isotopic and trace-element evidence for an endogenous Dupal mantle component. Chemical Geology 97, 47-63.

van Hattum, M.W.A., Hall, R., Pickard, A.L., Nichols, G.J., 2006. Southeast Asian sediments not from Asia: Provenance and geochronology of north Borneo sandstones. Geology 34, 589-592.

van Leeuwen, T., Allen, C.M., Kadarusman, A., Elburg, M., Palin, J.M., Muhardjo, Suwijanto, 2007. Petrologic, isotopic, and radiometric age constraints on the origin and tectonic history of the Malino Metamorphic Complex, NW Sulawesi, Indonesia. Journal of Asian Earth Sciences 29, 751-777.

Vroon, P.Z., Van Bergen, M.J., Klaver, G.J., White, W. M., 1995. Strontium, neodymium and lead isotopic and trace element signatures of the east Indonesian sediments – provenance and implications for Banda arc magma genesis. Geochimica et Cosmochimica Acta 59, 2573-2598.

Weis, D., Frey, F.A., 1996. Role of the Kerguelen plume in generating the eastern Indian Ocean seafloor. Journal of Geophysical Research 101, 13831-13849.

Wooden, J.L., Mueller, P.A., 1988. Pb, Sr, and Nd isotopic composition of a suite of Late Archean, igneous rocks, eastern Beartooth Mountains: implications for crust-mantle evolution. Earth and Planetary Science Letters 87, 59-72.

Figure Captions

Figure 1. (a) Map showing location of Borneo and other sites discussed with plate boundaries (thick solid lines) and major faults (dashed lines). Black box shows location of (b). Geographic features are noted in capitals. Locations of magmatic suites plotted in Figures 4, 5 and 9 are listed in italics. Abbreviations; H – Hose Mountains, K – Kelian, M – Metalung, N – Nuit, NP - North Palawan, U - Usun Apau. (b) Semporna peninsula in southeastern Sabah showing the distribution of Mio-Pliocene and Plio-Pleistocene magmatism after Kirk (1962), Haile et al. (1965), Leong (1974), Lim (1981), Lee (1988), Bellon and Rangin (1991) and Hutchison et al. (2000).

Figure 2. Plots of selected major elements versus MgO for Plio-Pleistocene lavas from Tawau (PP1 – PP4) and Mostyn.

Figure 3. Plots of selected trace elements versus MgO for Plio-Pleistocene lavas from Tawau (PP1 – PP4) and Mostyn.

Figure 4. N-MORB normalised multi-elements plots for Plio-Pleistocene lavas from Tawau and Mostyn. All normalisation factors from Sun and McDonough (1989).

Figure 5. Plots of (a) Nb/K, and (b) Nb/La, normalised to N-MORB, versus MgO for Plio-Pleistocene lavas from Tawau and Mostyn. Data for Kelian, central Borneo, from Chiang (2002).

Figure 6. Plots of (a) $^{87}Sr/^{86}Sr$, (b) $^{143}Nd/^{144}Nd$ and (c) $^{206}Pb/^{204}Pb$ versus MgO for Plio-Pleistocene lavas from Tawau and Mostyn. Mio-Pliocene arc data from Tawau from Chiang (2002).

Figure 7. (a) $^{143}Nd/^{144}Nd$ versus $^{87}Sr/^{86}Sr$, (b) $^{207}Pb/^{204}Pb$ versus $^{206}Pb/^{204}Pb$, (c) $^{208}Pb/^{204}Pb$ versus $^{206}Pb/^{204}Pb$, and (d) $^{143}Nd/^{144}Nd$ versus $^{206}Pb/^{204}Pb$ for Plio-Pleistocene lavas from Tawau and Mostyn. Comparison data shown for Indian MORB (GERM: http://earthref.org/GERM/); northern and central Sulu Arc (Castillo et al., 2007); Sulu and Celebes seafloor basalts (Spadea et al., 1996), Scarborough Seamounts and Reed Banks (Tu et al., 1992) and Hainan Island (Tu et al., 1991). Northern Hemisphere Reference Line in (b) and (c) from Hart (1984).

Figure 8. Comparison of $^{87}Sr/^{86}Sr$ versus $^{143}Nd/^{144}Nd$ of Plio-Pleistocene lavas from Semporna with assimilation with fractional crystallisation (AFC) models (DePaolo, 1981). In each case the uncontaminated melt has isotopic ratios and trace element concentrations of basalt SBK13. In all AFC models r = 0.15, except EIS 2 in which r = 0.85. Tick marks represent reduction of the fraction of melt remaining by 0.1, except for EIS 2 where ticks are shown for 0.99, 0.98 and 0.95 of original melt. Partition coefficients are 1.5 for Sr and 0.1 for Nd (GERM: http://earthref.org/GERM/). The contaminants for each model are: LC 1, $^{87}Sr/^{86}Sr$ = 0.709259, $^{143}Nd/^{144}Nd$ = 0.512304, Sr = 252ppm and Nd = 23.2ppm (Capoas granite, Palawan; Encarnación and Mukasa, 1997); EIS 1 and 2, $^{87}Sr/^{86}Sr$ = 0.739404, $^{143}Nd/^{144}Nd$ = 0.511984, Sr = 114ppm and Nd = 38.1ppm (East Indonesian Sediment; Vroon et al., 1995); AC 1, $^{87}Sr/^{86}Sr$ = 0.72460, $^{143}Nd/^{144}Nd$ = 0.51025, Sr = 400ppm and Nd = 43.1ppm (Beartooth Mountains, USA; Wooden and Mueller, 1988); AC2, $^{87}Sr/^{86}Sr$ = 0.70890, $^{143}Nd/^{144}Nd$ = 0.51041, Sr = 573ppm and Nd = 28.8ppm (Archean migmatite from Lofoten-Verterålen, Norway; Jacobsen and Wasserburg, 1978).

Figure 9. (a) OIB normalised multi-elements plots for mafic lavas from Semporna, northern Sulu Arc, Reed Bank and Hainan Island. (b) ^{143}Nd/^{144}Nd versus Zr/Nb for high-Nb basalts from Semporna peninsula, Sulu Arc and South China Sea sites. Data sources as in Fig. 7.

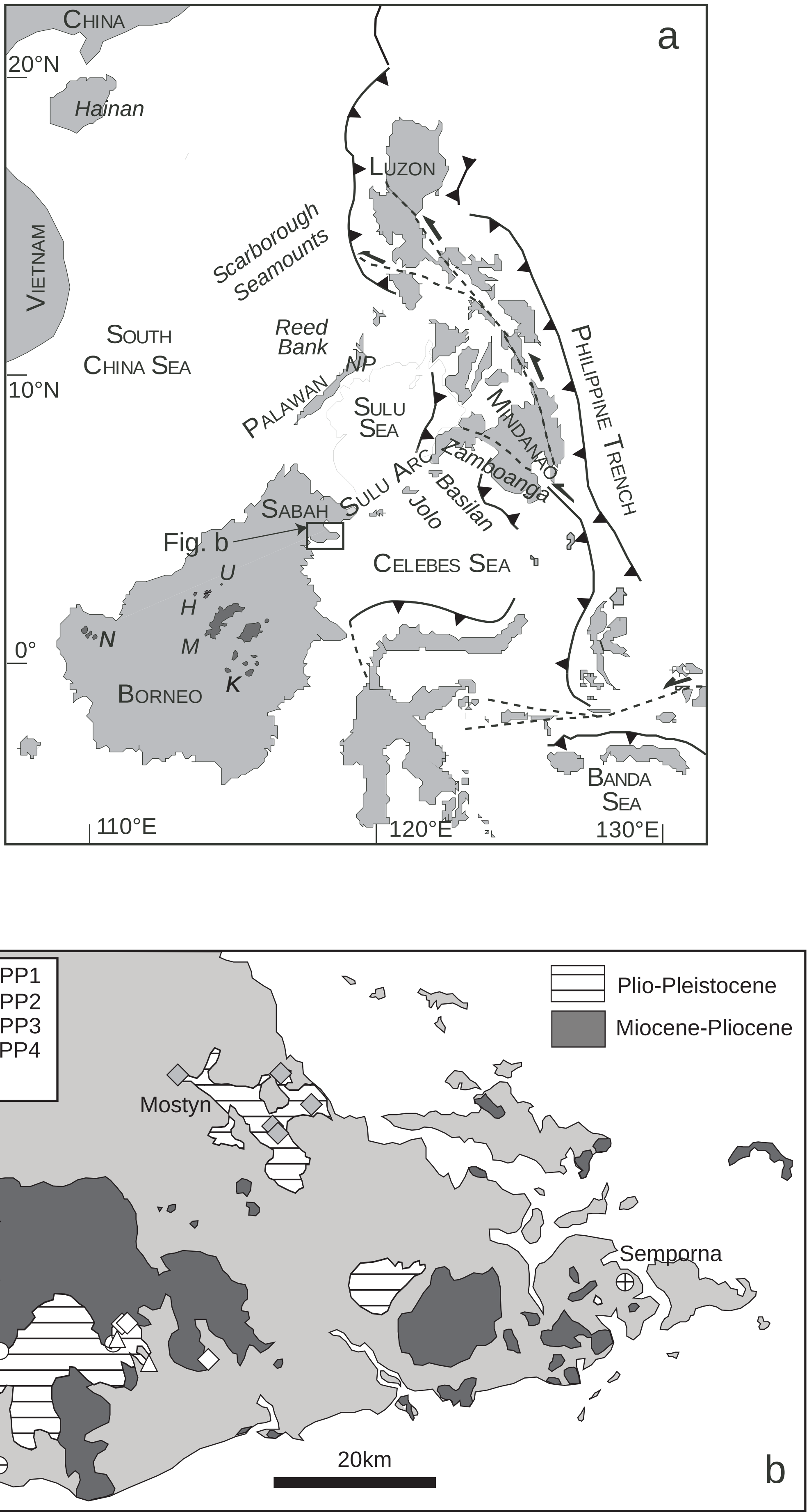
a
CHINA
20°N
Hainan
LUZON
Scarborough
Seamounts
VIETNAM
SOUTH
CHINA SEA
Reed
Bank
NP
10°N
PALAWAN
SULU
SEA
MINDANAO
PHILIPPINE TRENCH
Zamboanga
SULU ARC
Basilan
Jolo
SABAH
Fig. b
CELEBES SEA
U
H
N
M
0°
K
BORNEO
BANDA
SEA
110°E
120°E
130°E
Tawau PP1
Tawau PP2
Tawau PP3
Tawau PP4
Mostyn
Plio-Pleistocene
Miocene-Pliocene
Mostyn
Semporna
Tawau
20km
b

Figure 1

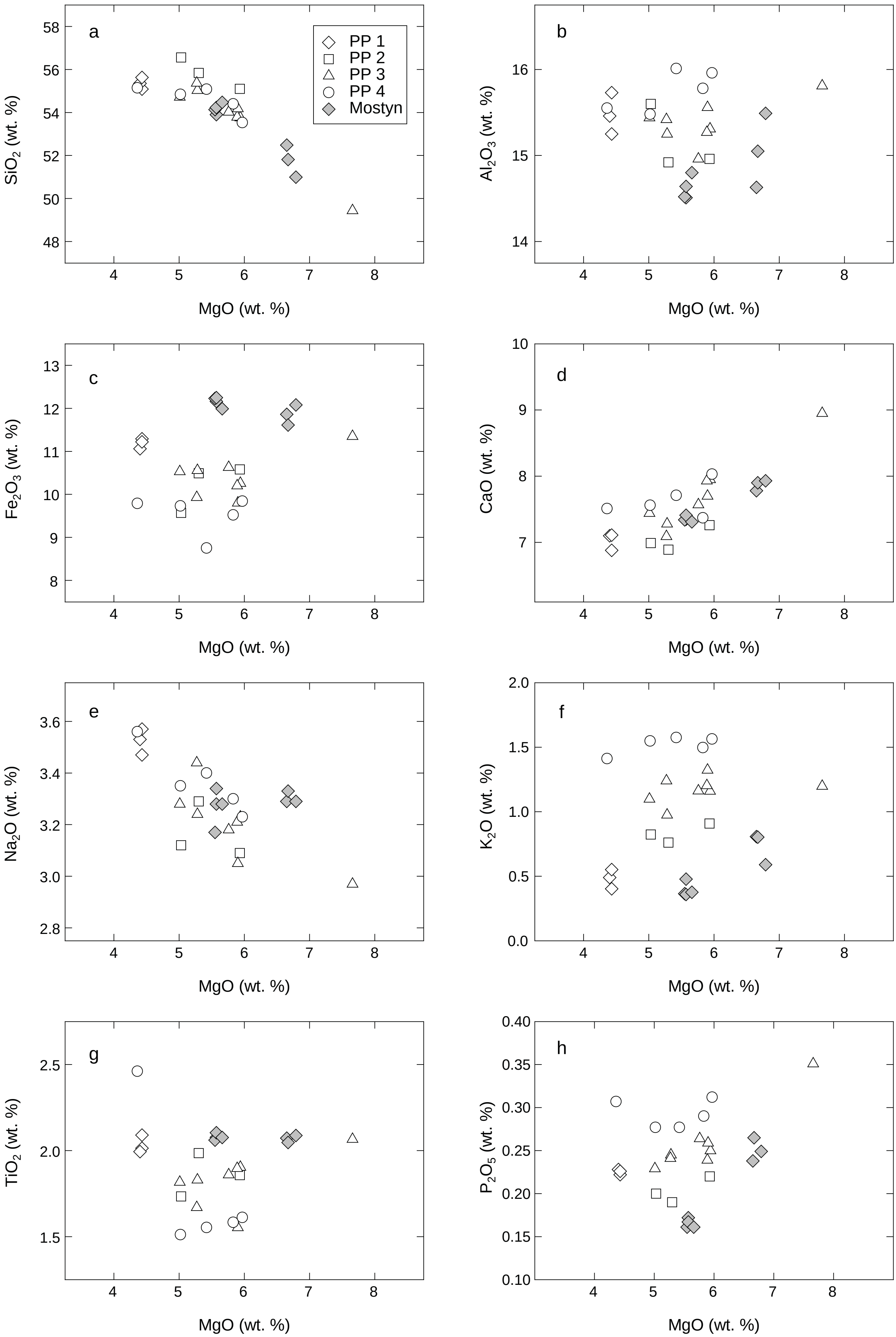

a
b
c
d
e
f
g
h
PP 1
PP 2
PP 3
PP 4
Mostyn
SiO2 (wt. %)
Al2O3 (wt. %)
Fe2O3 (wt. %)
CaO (wt. %)
Na2O (wt. %)
K2O (wt. %)
TiO2 (wt. %)
P2O5 (wt. %)
MgO (wt. %)

Figure 2

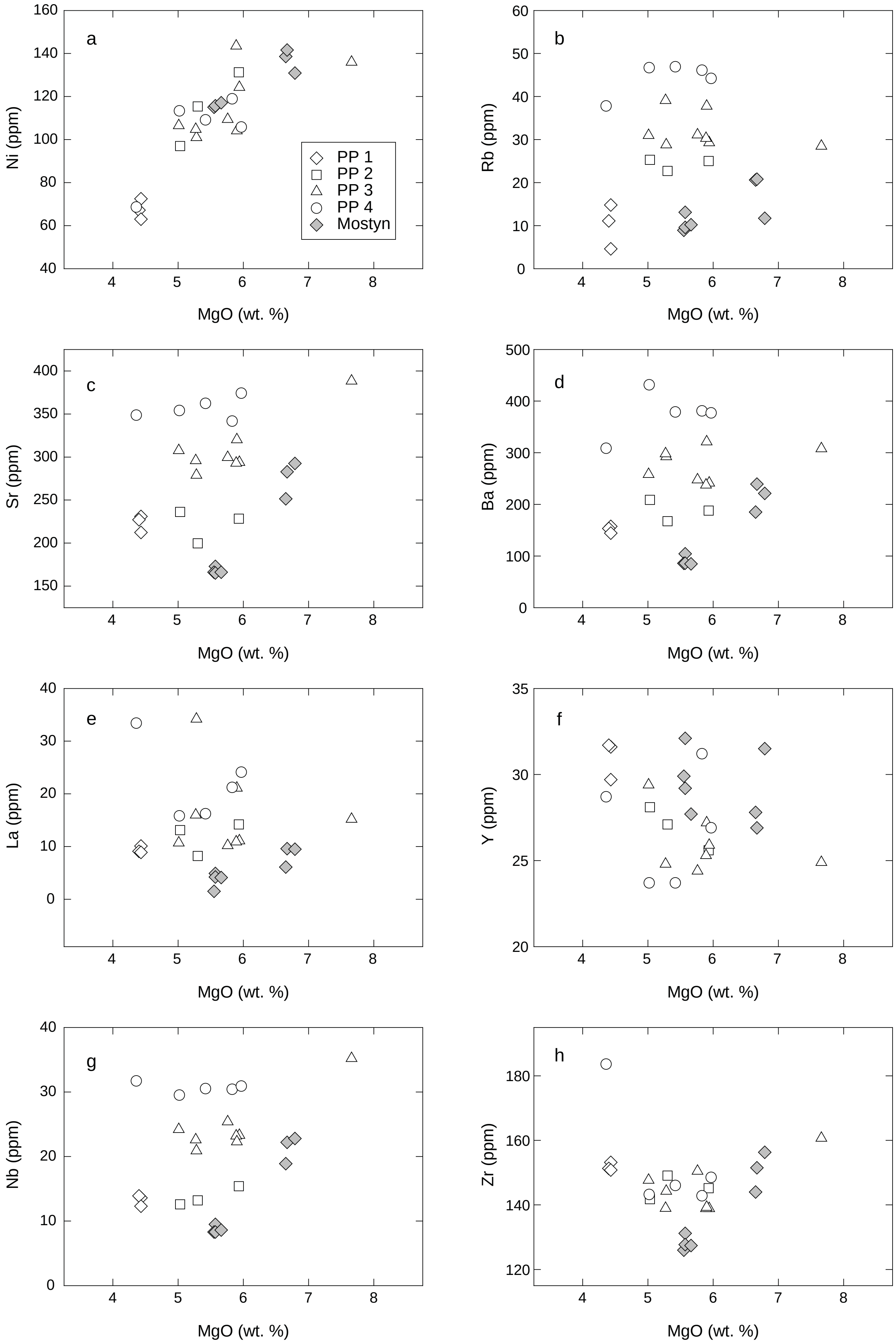

a
b
c
d
e
f
g
h
Ni (ppm)
Rb (ppm)
Sr (ppm)
Ba (ppm)
La (ppm)
Y (ppm)
Nb (ppm)
Zr (ppm)
MgO (wt. %)
PP 1
PP 2
PP 3
PP 4
Mostyn

Figure 3

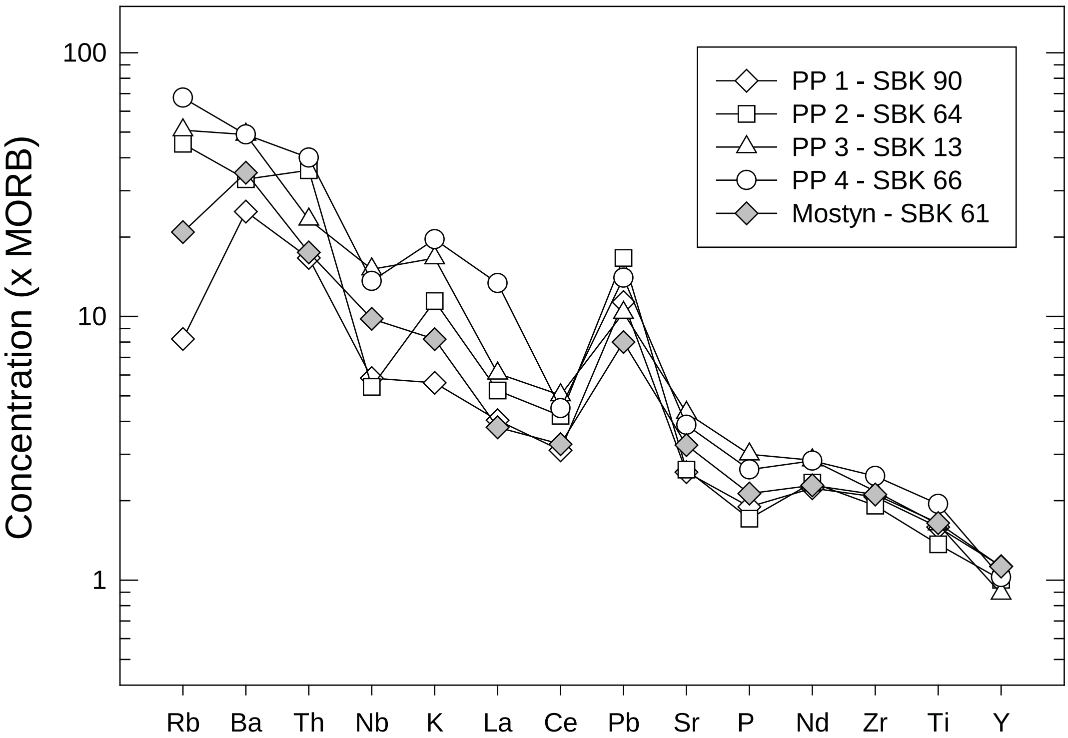

Concentration (x MORB)
100
10
1
PP 1 - SBK 90
PP 2 - SBK 64
PP 3 - SBK 13
PP 4 - SBK 66
Mostyn - SBK 61
Rb
Ba
Th
Nb
K
La
Ce
Pb
Sr
P
Nd
Zr
Ti
Y

Figure 4

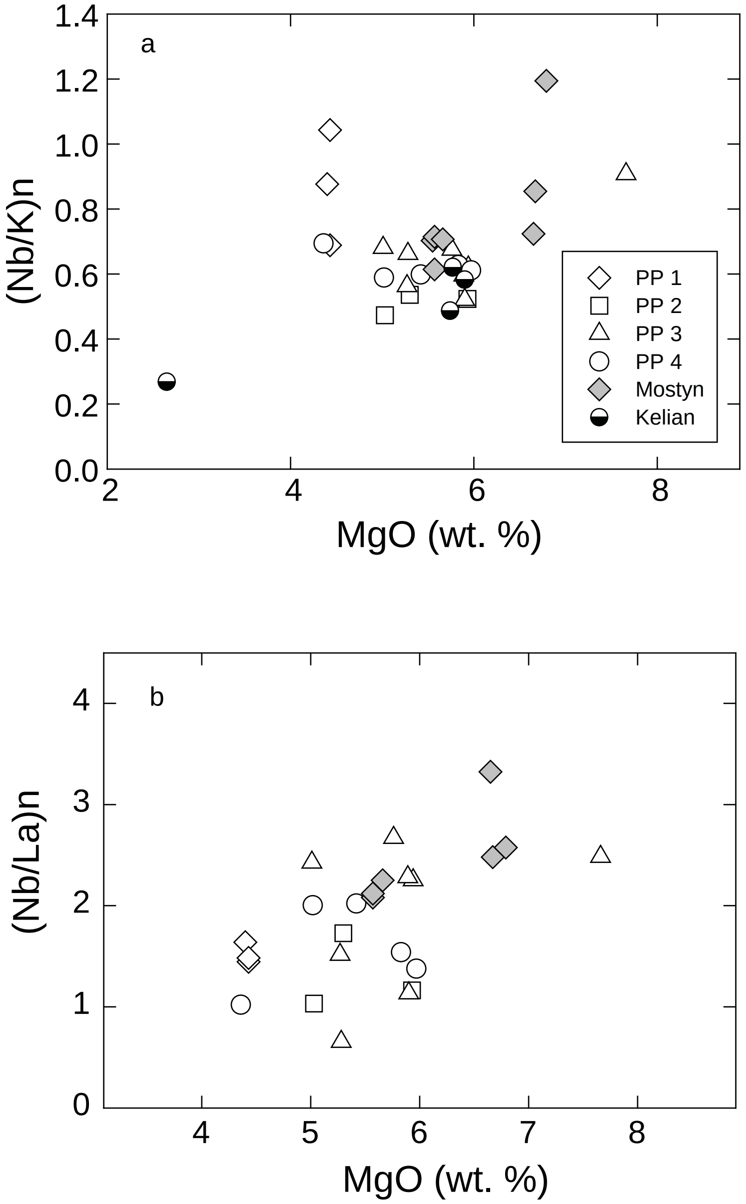
a
b
(Nb/K)n
(Nb/La)n
MgO (wt. %)
MgO (wt. %)
PP 1
PP 2
PP 3
PP 4
Mostyn
Kelian
0.0
0.2
0.4
0.6
0.8
1.0
1.2
1.4
2
4
6
8
0
1
2
3
4
4
5
6
7
8

Figure 5

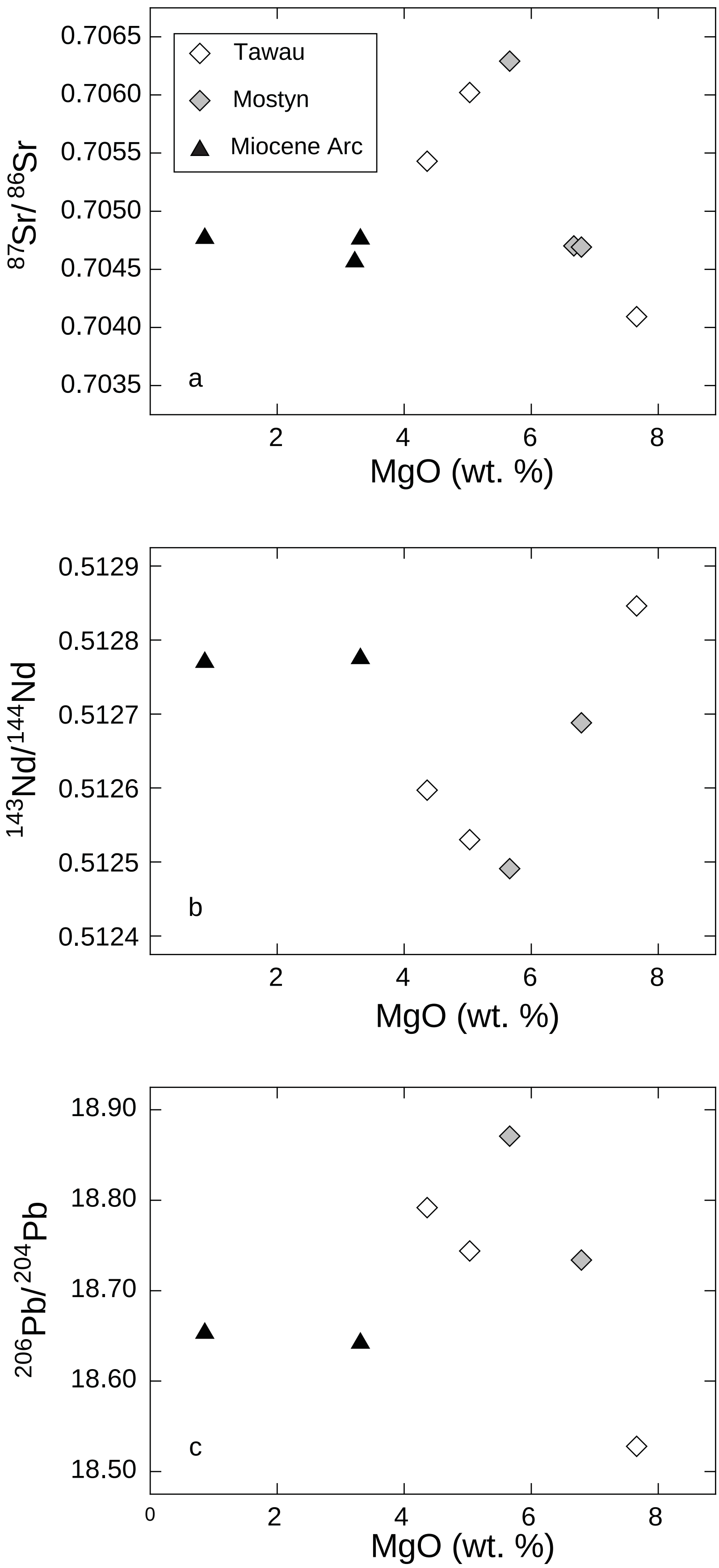
Tawau
Mostyn
Miocene Arc
$^{87}Sr/^{86}Sr$
0.7065
0.7060
0.7055
0.7050
0.7045
0.7040
0.7035
a
2
4
6
8
MgO (wt. %)
$^{143}Nd/^{144}Nd$
0.5129
0.5128
0.5127
0.5126
0.5125
0.5124
b
2
4
6
8
MgO (wt. %)
$^{206}Pb/^{204}Pb$
18.90
18.80
18.70
18.60
18.50
c
0
2
4
6
8
MgO (wt. %)

Figure 6

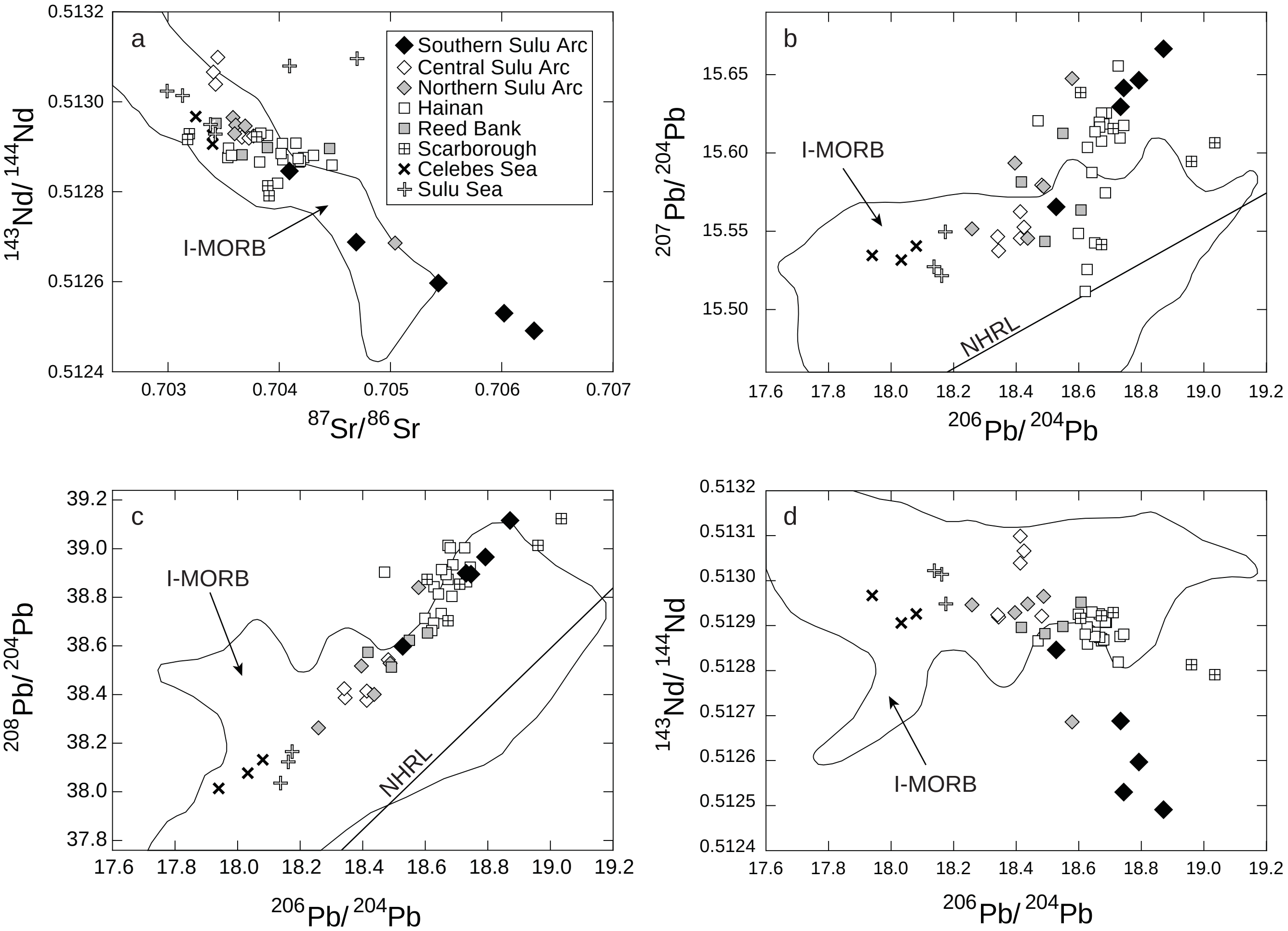

a
b
c
d
Southern Sulu Arc
Central Sulu Arc
Northern Sulu Arc
Hainan
Reed Bank
Scarborough
Celebes Sea
Sulu Sea
I-MORB
NHRL
143Nd/144Nd
87Sr/86Sr
207Pb/204Pb
206Pb/204Pb
208Pb/204Pb

Figure 7

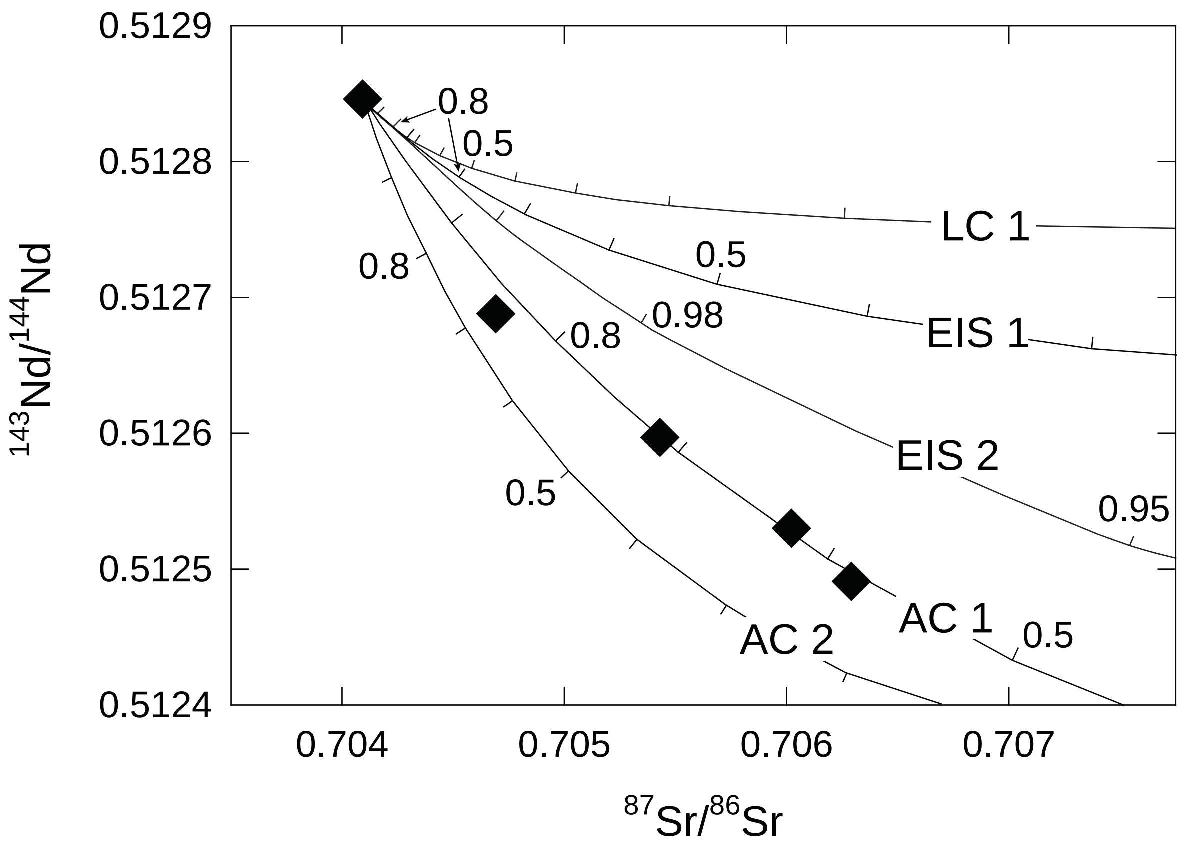
0.5129
0.5128
0.5127
0.5126
0.5125
0.5124
0.704
0.705
0.706
0.707
$^{143}Nd/^{144}Nd$
$^{87}Sr/^{86}Sr$
0.8
0.5
LC 1
0.5
EIS 1
0.8
0.98
0.8
EIS 2
0.95
0.5
AC 1
0.5
AC 2

Figure 8

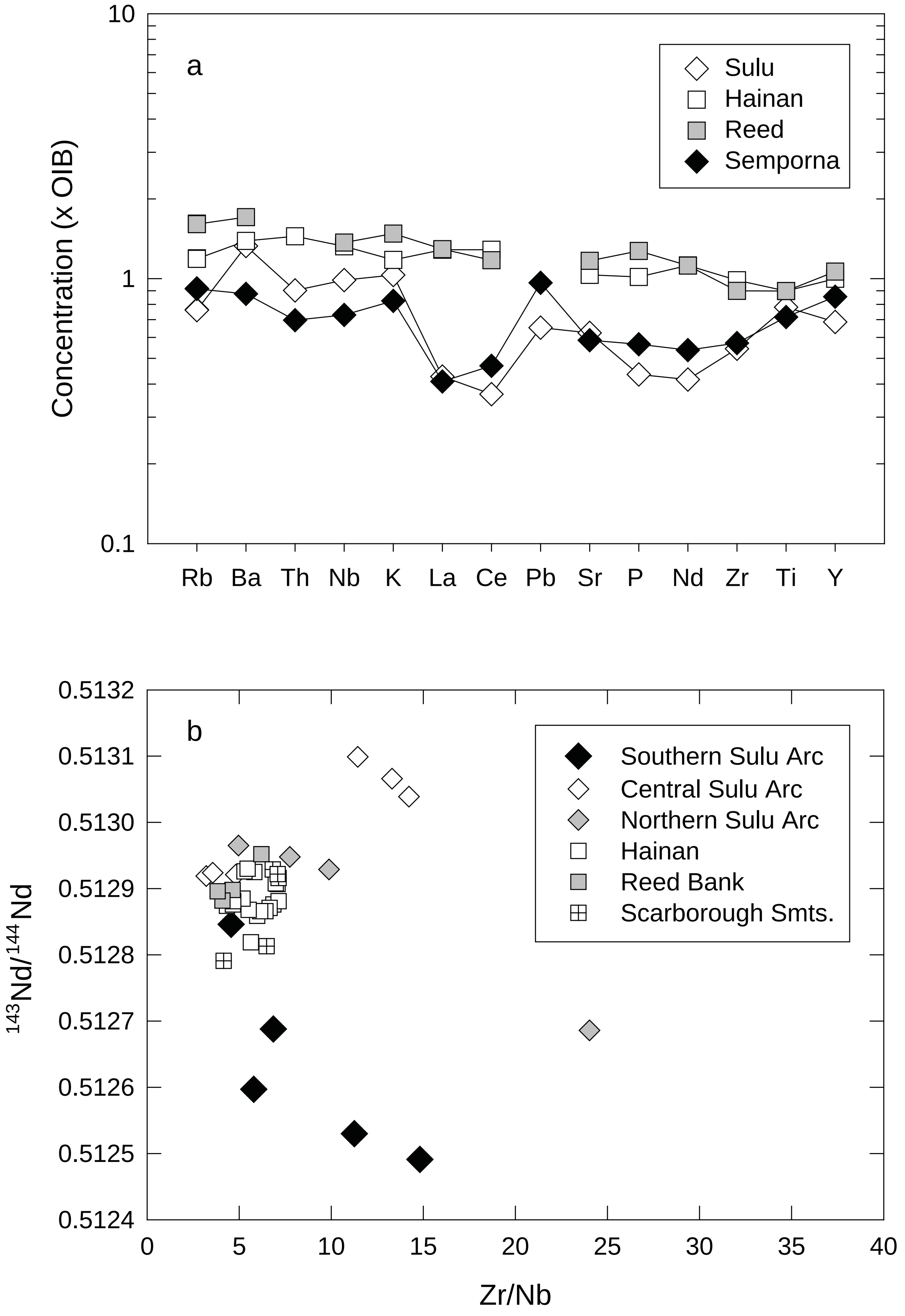

10
1
0.1
a
Sulu
Hainan
Reed
Semporna
Concentration (x OIB)
Rb
Ba
Th
Nb
K
La
Ce
Pb
Sr
P
Nd
Zr
Ti
Y
0.5132
0.5131
0.5130
0.5129
0.5128
0.5127
0.5126
0.5125
0.5124
b
Southern Sulu Arc
Central Sulu Arc
Northern Sulu Arc
Hainan
Reed Bank
Scarborough Smts.
143Nd/144Nd
0
5
10
15
20
25
30
35
40
Zr/Nb

Figure 9

Table 1. Major and trace element concentrations in Plio-Pleistocene lavas from the Semporna Peninsula.

	Tawau SBK3	Tawau SBK5	Tawau SBK6	Tawau SBK7	Tawau SBK13	Tawau SBK64	Tawau SBK65	Tawau SBK66	Tawau SBK67	Tawau SBK68	Tawau SBK69	Tawau SBK70	Tawau SBK71
SiO_2 (wt.%, ± 0.16)	55.08	54.84	54.02	54.72	49.44	56.56	55.84	55.14	55.03	55.37	53.76	53.79	55.10
TiO_2 (wt.%, ± 0.010)	1.55	1.51	1.86	1.82	2.07	1.73	1.99	2.46	1.83	1.67	1.90	1.90	1.86
Al_2O_3 (wt.%, ± 0.07)	16.01	15.48	14.96	15.44	15.81	15.60	14.92	15.55	15.25	15.42	15.31	15.27	14.96
Fe_2O_3 (wt.%, ± 0.10)	8.75	9.73	10.63	10.53	11.35	9.57	10.49	9.79	10.56	9.93	10.26	10.20	10.58
MgO (wt.%, ± 0.07)	5.42	5.02	5.76	5.01	7.66	5.03	5.30	4.36	5.28	5.27	5.94	5.89	5.93
MnO (wt.%, ± 0.006)	0.14	0.23	0.15	0.14	0.17	0.14	0.14	0.14	0.17	0.14	0.15	0.14	0.14
CaO (wt.%, ± 0.03)	7.71	7.56	7.57	7.44	8.95	6.99	6.89	7.51	7.28	7.09	7.95	7.93	7.26
Na_2O (wt.%, ± 0.13)	3.40	3.35	3.18	3.28	2.97	3.12	3.29	3.56	3.24	3.44	3.23	3.21	3.09
K_2O (wt.%, ± 0.010)	1.58	1.55	1.16	1.10	1.20	0.82	0.76	1.41	0.98	1.24	1.16	1.20	0.91
P_2O_5 (wt.%, ± 0.007)	0.28	0.28	0.26	0.23	0.35	0.20	0.19	0.31	0.25	0.24	0.25	0.24	0.22
Total	99.91	99.55	99.56	99.70	99.97	99.76	99.80	100.24	99.86	99.81	99.91	99.77	100.04
LOI	-0.44	0.20	-0.39	0.20	0.84	0.11	-0.49	-0.20	0.01	-0.43	-0.21	-0.47	-0.10
Mg#	55.1	50.6	51.8	48.5	57.2	51.0	50.0	46.9	49.8	51.2	53.4	53.3	52.6
Ni (ppm, ± 1.0)	109.1	113.3	109.4	106.5	136.0	97.0	115.4	68.6	101.0	104.8	124.3	143.5	131.3
Cr (± 1.0)	168.8	160.7	159.4	154.5	231.2	164.8	188.7	73.9	151.6	153.3	202.9	203.1	218.9
V (± 1.0)	149.9	144.6	151.6	156.9	240.1	160.0	159.8	171.9	141.5	140.3	165.2	165.8	165.2
Sc (± 0.6)	19.1	19.3	19.8	20.2	25.5	19.6	19.6	20.8	19.4	19.1	21.7	22.5	22.1
Cu (± 1.0)	44.3	42.3	46.5	35.8	61.3	46.1	46.2	45.7	47.4	46.8	57.1	56.9	51.2
Zn (± 0.8)	94.2	90.8	106.7	110.6	106.2	104.7	116.0	110.2	104.7	99.6	112.4	110.8	109.6
Cl (± 50)	409	170	63	97				206	163	189	204	236	114
Ga (± 0.7)	20.3	18.8	18.9	20.1	21.1	21.3	21.0	20.9	20.3	20.1	21.4	20.1	19.3
Ba (± 3)	379	432	248	258	308	209	167	308	293	298	242	238	188
Rb (± 0.4)	46.9	46.7	31.1	31.0	28.5	25.3	22.7	37.8	28.8	39.1	29.3	30.3	25.0
Sr (± 0.6)	362.3	353.9	299.7	307.6	388.4	236.2	199.8	348.6	279.0	296.0	293.9	293.0	228.3
Zr (± 0.6)	146.0	143.2	150.5	147.7	160.7	141.8	149.1	183.6	144.3	139.0	138.9	138.9	145.2
Nb (± 0.3)	30.5	29.5	25.4	24.2	35.2	12.6	13.2	31.7	20.9	22.6	23.3	23.2	15.4
Y (± 0.4)	23.7	23.7	24.4	29.4	24.9	28.1	27.1	28.7	65.8	24.8	25.9	25.3	25.6
La (± 1.0)	16.2	15.8	10.2	10.7	15.2	13.1	8.2	33.4	34.2	16.0	11.1	10.9	14.2
Ce (± 3.0)	33.6	35.4	25.8	26.5	37.7	31.5	24.5	33.6	33.5	26.3	26.5	25.5	29.6
Nd (± 0.7)	18.4	18.8	16.0	17.2	20.8	17.1	15.7	20.7	41.3	16.3	16.3	15.7	17.0
Pb (± 0.9)	4.5	5.9	2.6	4.8	3.1	5.0	4.4	4.2	3.1	4.1	2.9	3.3	5.3
Th (± 0.7)	4.4	4.0	2.7	3.4	2.8	4.3	4.4	4.8	2.4	3.8	3.7	2.3	5.9

Table 1 (cont.).

	Tawau SBK72	Tawau SBK90	Tawau SBK91	Tawau SBK92	Tawau SBK93	Tawau SBK94	Mostyn SBK30	Mostyn SBK31	Mostyn SBK60	Mostyn SBK61	Mostyn SBK62	Mostyn SBK63	Mostyn SA9802
SiO_2 (wt.%)	54.40	55.09	55.35	55.63	54.18	53.53	53.90	52.48	51.81	50.99	54.13	54.23	54.47
TiO_2	1.58	2.01	1.99	2.09	1.55	1.61	2.08	2.07	2.05	2.09	2.06	2.10	2.08
Al_2O_3	15.78	15.73	15.46	15.25	15.56	15.96	14.51	14.63	15.05	15.49	14.52	14.64	14.80
Fe_2O_3	9.52	11.29	11.06	11.22	9.80	9.84	12.16	11.86	11.61	12.08	12.23	12.25	11.99
MgO	5.83	4.43	4.40	4.43	5.90	5.97	5.57	6.65	6.67	6.79	5.55	5.57	5.66
MnO	0.15	0.13	0.15	0.15	0.14	0.14	0.16	0.15	0.16	0.17	0.14	0.16	0.16
CaO	7.37	6.88	7.10	7.11	7.70	8.03	7.35	7.78	7.90	7.93	7.34	7.41	7.31
Na_2O	3.30	3.47	3.53	3.57	3.05	3.23	3.34	3.29	3.33	3.29	3.17	3.28	3.28
K_2O	1.50	0.40	0.49	0.55	1.32	1.56	0.48	0.81	0.80	0.59	0.37	0.36	0.38
P_2O_5	0.29	0.22	0.23	0.23	0.26	0.31	0.17	0.24	0.27	0.25	0.16	0.17	0.16
Total	99.71	99.66	99.77	100.22	99.46	100.18	99.73	99.97	99.65	99.66	99.67	100.17	100.29
LOI	-0.07	0.77	0.03	-0.53	0.07	0.04	-0.50	-0.70	-0.44	0.13	-0.44	-0.59	-0.34
Mg#	54.8	43.8	44.1	43.9	54.4	54.6	47.6	52.6	53.2	52.7	47.3	47.4	48.3
Ni (ppm)	118.9	72.5	67.2	63.0	104.1	105.8	115.6	138.6	141.6	130.9	115.0	115.7	117.1
Cr	178.9	120.3	122.5	114.1	177.3	193.5	186.2	214.9	219.3	218.2	192.3	190.1	191.9
V	148.2	154.3	153.1	147.9	160.1	165.2	164.8	163.0	167.1	173.3	164.5	164.6	164.9
Sc	19.9	21.1	20.1	19.9	21.1	21.6	21.2	21.2	22.3	23.5	22.1	23.6	22.6
Cu	47.3	39.8	40.8	45.1	44.2	44.6	47.1	51.2	51.2	47.5	45.3	45.7	48.6
Zn	88.4	119.5	120.6	114.0	98.4	93.2	123.2	115.1	115.1	112.9	122.1	122.0	116.2
Cl	181		7		150	215	94	165	134	115			
Ga	20.2	21.6	22.3	21.6	18.7	20.8	20.8	20.9	20.8	21.0	20.3	21.8	21.0
Ba	381	157	153	144	321	377	104	185	239	221	86	86	85
Rb	46.1	4.6	11.1	14.8	37.8	44.2	13.1	20.6	20.8	11.7	8.9	9.6	10.2
Sr	341.7	231.0	227.2	212.4	320.3	374.1	172.9	251.4	282.8	292.5	166.2	165.3	166.2
Zr	142.8	153.2	151.3	150.8	139.3	148.5	131.2	144.0	151.5	156.3	126.0	127.7	127.4
Nb	30.4	13.6	13.9	12.3	22.3	30.9	9.5	18.9	22.2	22.8	8.3	8.3	6.8
Y	31.2	31.6	31.7	29.7	27.2	26.9	32.1	27.8	26.9	31.5	29.9	29.2	27.7
La	21.2	10.1	9.1	8.9	21.1	24.1	4.9	6.1	9.6	9.5	1.5	4.2	4.1
Ce	35.0	23.3	23.1	22.6	36.7	41.6	15.1	19.3	24.7	24.6	13.6	11.2	14.5
Nd	20.6	16.3	17.5	15.5	20.9	24.4	12.6	14.5	15.5	16.7	11.7	11.1	12.3
Pb	4.8	3.4	4.1	2.4	5.7	5.7	2.8	1.8	2.4	2.4	2.6	2.7	2.0
Th	4.6	2.0	2.8	2.8	5.8	6.3	1.4	2.6	2.9	2.1	1.5	1.3	1.9

Table 2. Isotopic ratios of Plio-Pleistocene lavas from the Semporna Peninsula.

	$^{87}Sr/^{86}Sr$	$^{143}Nd/^{144}Nd$	$^{206}Pb/^{204}Pb$	$^{207}Pb/^{204}Pb$	$^{208}Pb/^{204}Pb$
SBK13	0.704092	0.512846	18.528	15.566	38.598
SBK64	0.706021	0.512530	18.744	15.642	38.895
SBK66	0.705430	0.512597	18.792	15.647	38.966
SBK60	0.704701				
SBK61	0.704691	0.512688	18.734	15.630	38.899
SA9802	0.706291	0.512491	18.871	15.667	39.116